EXPERIMENTAL AND NUMERICAL STUDY OF HEAT TRANSFER PHENOMENON IN A MICRO DROPLET REACTOR

by

CHINTAN JITENDRA GANDHI

Presented to the Faculty of the Graduate School of

The University of Texas at Arlington in Partial Fulfillment

of the Requirements

for the Degree of

MASTER OF SCIENCE IN MECHANICAL ENGINEERING

THE UNIVERSITY OF TEXAS AT ARLINGTON

December 2016

ACKNOWLEDGEMENTS

I like to dedicate this thesis to my mother, because of her love and blessings I have reach so far and completed my work successfully. My father and my brother has always been a source of inspiration for me, they always taught me to never give up in any situation.

I am grateful to my advisor Dr. Hyejin Moon for providing an opportunity to accomplish Master's Thesis under her guidance, not only that she also gave me a chance to utilize UTA NanoFab and other facilities to simulate my research work. It is said that "the essence of independent mind lies what it thinks but in how it thinks". She always believes in independent thinking which helps me to change my perception about brain storming process. Her guidance helped me in all the time of research and writing of this thesis. I could not have imagined having a better advisor and mentor for my Master's Thesis study. I doubt that I will ever be able to convey my appreciation fully, but I owe her my eternal gratitude. A big thank you to our committee members, Dr. Miguel Amaya, Dr. Hyejin Moon and Dr. Donghyun Shin for their support and valuable feedback.

It's my honor to be a part of Integrated Micro Nano fluidics laboratory. I would take an opportunity to thank my fellow labmates Ali Farzbood, Kunjan Chaudhari, Shubodeep Paul, Viraj, Matin in for the stimulating discussions and helping me throughout my research work. My special thanks to MunMun Nahar, for helping me in the computational and numerical study. I also like to convey gratitude to Arvind Venketesan for helping me in my experimental setup. At last I would like to express my vote of appreciation to my roommates and my group of friends who always supported throughout my journey.

December, 2016

ABSTRACT

EXPERIMENTAL AND NUMERICAL STUDY OF HEAT TRANSFER PHENOMENON IN MICRO DROPLET REACTOR

Chintan Jitendra Gandhi, MS

The University of Texas at Arlington, 2016

Supervising Professor: Hyejin Moon

Temperature is an important control parameter during chemical reaction process. Micro reactors have attracted much attention due to its capability of excellent heat and mass transfer, fast reaction, and inherent safety of small scale. Among various types of micro reactors, micro droplet as a batch reactor has its own advantages such as high multiplexing capability. However, strong heat dissipation characteristics of microscale systems (due to large surface to volume ratio) hampers the measurement and monitor of enthalpy changes during the reaction.

This study mainly focuses on temperature monitoring at micro droplet reactor by using thin film resistance temperature detector (RTD). Indium tin oxide (ITO), optically transparent and electrically conductive material was used to fabricate a RTD. A simple reaction was carried out on (EWOD) digital microfluidic device. Droplets of strong base and strong acid were dispensed on an electrode with embedded ITO RTD, and they were allowed to react. This exothermic reaction released considerable amount of heat during reaction which was monitored by RTD temperature measurement. Due to high heat dissipation, very small temperature rise was observed because experiment was not carried out in a control environment. Multi-physics numerical modeling was carried out to

determine the amount of overall heat loss through conduction, convection and evaporation. The numerical results were compared with the experimental data to examine the difference in heat transfer and evaporation rate.

TABLE OF CONTENTS

LIST OF ILLUSTRATIONS

LIST OF TABLES

Chapter 1

INTRODUCTION

A micro reactor is generally defined as a device consisting of a number of interconnecting micro channels in which small quantities of reagents are manipulated, mixed and allowed to react for a specified period of time [1]. The movement of fluids can be achieved in a number of ways with the most common being mechanical Micro pumping, Electrowetting on dilectric (EWOD) droplet flow and electroosmotic flow (EOF). EWOD devices are special versatile platform for chemical synthesis at the microscale [2]. The varieties of chemicals are capable of moving on EWOD platform and they are compatible with a wide range of chemicals and temperatures, their special structure enable various chemical processes which are critical in multi-step reaction schemes, and the use of small volumes (in µL) permits optimizations that can lead to reduced synthesis and reaction time [2]. However, it is difficult to estimate exact reaction time at micro scale unlike macro scale which is determined with the help of reaction kinetics. The importance of study heat transfer phenomenon at microscale in the context of chemical reactions cannot be understated as it is helpful in designing the microsystem. At microscale it is quite difficult to sense the exact temperature change at atmospheric conditions because of very large surface area to volume ratio, which eventually increases heat losses. Hence, cheap and reliable embedded thin film temperature, heat flux sensors were developed to sense heat at micro scale.

1.1 Temperature Sensing with thin film resistance temperature detectors(RTD)

Thin-film technology has been found to be appropriate for temperature measurement in micro system because their deposition thickness is in the range of 200-100 nm and their relative locations are very accurate as they are obtained from the SI/IC

fabrication photolithography mask patterns. Certain metals like platinum, gold and nickel possesses linear temperature versus resistance characteristics under certain temperature limit. Platinum is one of the most common metal for RTD. There are many advantages of using thin film RTD, including precision, long-term stability, and good hysteresis characteristics.

However, in previous research [3] of hot spot cooling it was found that, instead of using thin films of these expensive metals such as platinum and gold, a conductive ceramic material indium tin oxide (ITO) can also be used as an RTD for temperature ranges of 100°C. Figure 1-1 shows the calibration curve of ITO RTD from room temperature to 100°C temperature range.

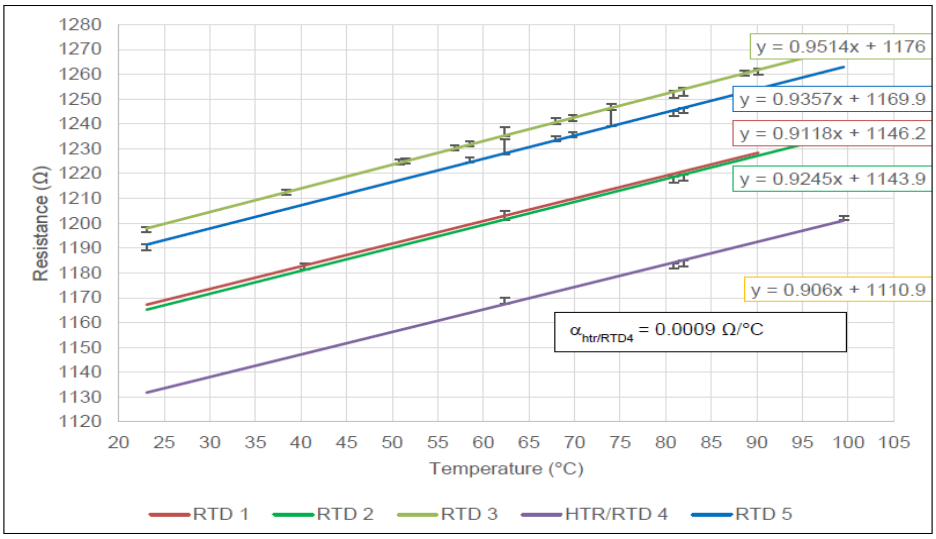

Figure 1-1 Calibration of ITO RTD [3]

There are several advantages of using ITO as a thin film RTD. ITO is having linear and repeatable temperature versus resistance curve under 100 °C with good sensitivity. Also it is conductive and optically transparent which extend their application in

area of microfluidics. Most important advantage of ITO is that it is quiet cheaper than platinum and its fabrication of thin film RTD is also very easy.

1.2 Heat Transfer at Micro scale

For transient heat transfer there is a dimensionless number called Biot number, which is the ratio of convection at the surface of the body at microscale to the conduction with in the body [4]. The physical significance of Biot number can be understood by imagining the heat flow from a small hot body subjected, to the surrounding fluid [4]. The heat flow experiences two resistances: the first within the body itself (which is influenced by both the size and composition of the body), and the second at the surface of the small body. If the thermal resistance of the fluid and body interface exceeds that thermal resistance offered by the interior of the body, the Biot number will be less than one.

For micro systems the Biot number can be considered to be less than 0.1 because of its small characteristic length for a microsystem body. For example, let's take 1 µL of a heated droplet. If we consider the droplet as spherical then its characteristic length would be $L_c = r/3$. The heat transfer coefficient was assumed to be 10 W/m^2-K in this case and conductivity of water is 0.6 W/m-K.

.

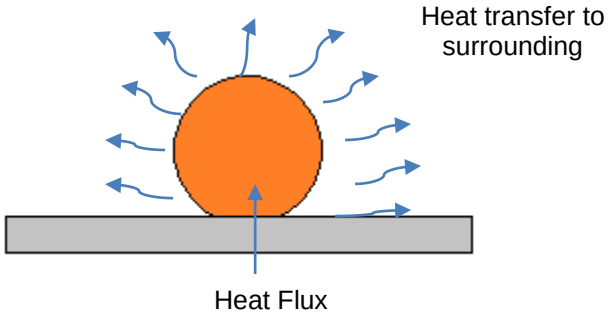

Figure 1.2 Heat transfer in a Micro Droplet

$$\text{Biot Number (Bi)} = \frac{\text{Convection at surface of the body}}{\text{Conduction within the surface of the body}}$$

$$Bi = \frac{h\ Lc\ \Delta T}{k\ \Delta T} = \frac{10 \times 0.00024}{0.6}$$

$$= 0.0034 << 0.1$$

Where,

h = convective heat transfer coefficient, = 10 W/m^2-K

k = thermal conductivity of the body= 0.6 W/m-K

L_c = characteristics length (volume of body by surface area)

= (0.62×10^{-3}) /3

= 0.00024 m

It can be interpreted from the Biot value that even though if convective heat transfer coefficient value is increased the Biot number value still remains less than 0.1. Since the Biot number is very small so the interior of the system may be assumed to have the same temperature at every point, although this temperature may be changing, as heat loss from the body at microscale from the surface but overall average temperature inside the droplet is most likely to be isothermal at any point of time.

CHAPTER 2 LITERATURE REVIEW AND GOALS OF RESEARCH

Since last some years microreactors have gained rapid development in carrying out efficiently numerous chemical synthesis, out of which the exothermic and endothermic reactions are considered to be one of the most suited reactions in microreactors [5-6]. Due to the characteristics of fast mixing, increased safety can handle reactions that are too exothermic or explosive to run at macro scale, excellent heat and mass transfer, and inherent safety in microreactors, it can bring many advantages high selectivity, better process control and faster reaction rate with system integration and automation. Out of all chemical reactions fast exothermal reactions are most suited for micro scale. Many fast and exothermic reactions have been performed in micro reactors such as fluorination [7], nitration [8] and rearrangement [9,10] reactions. For such reactions, it was a great challenge to determine a precise reaction enthalpy and temperature profiles in microreactors which are crucial to control the reaction process and perform the process design. However, it is difficult to get these heat transfer information with conventional equipment considering the very few µL of volume in a microreactors.

In the previous research of microscale heat engine, [11] it was found that at a microscale a thin thermal boundary layer will result large heat transfer. The thermal boundary layers are very thin which result in higher heat transfer per unit area. The heat transfer at wall can act differently at microscale. The Biot no (Bi) is the dimensionless parameter which is the ratio of convective heat transfer through the surface of the body to conductive heat transfer at its surface. [11] The numerical value of Biot Number (Bi) is a criterion which gives a direct indication of the relative importance of conduction and convection in determining the temperature distribution of a body being heated or cooled

by convection at its surface. [12] Convective heat transfer per unit area through the body is inverse of square length scale and conduction heat transfer per unit area is inverse of length scale. So if the length scale decreases the rate at which the temperature rises within the body is more compare to which is convected from the body into surrounding fluid. Thus, temperature gradient within the body at microscale is considered nearly zero at any time. Thus the relative heat losses at surface of the body potentially affect the chemical reaction and other processes occurring at microscale.

PDMS (polydimethylsiloxane) block [13] including a T-type microchannel and underneath a borosilicate substrate instrumented with gold thin film temperature sensors Figure 2-1 was fabricated to estimate enthalpy of reactions. A 1 mm thick aluminum plate and a 0.1 mm PDMS layer help to provide a constant temperature along the fluid flow direction. The strong acid and strong base of certain molarity were used as working fluids, that is HCL and NaOH solutions, are delivered into the microchannel at different flow rates. The microchannel width and height was 0.5mm and 50 mm. The maximum temperature rise was observed was 14^{o}C depending upon flow rate. Several 85nm of gold thermoresistance was used for temperature sensing after proper calibration. [13] These thermoresistance was fabricated using MEMS photolithography after depositing the desired thickness of gold on glass wafer.

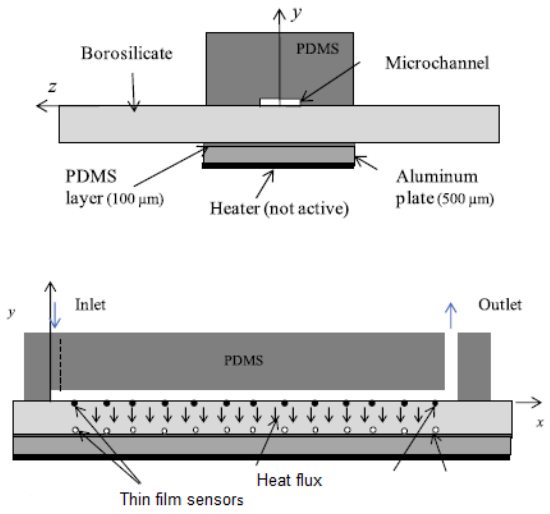

Figure 2-1 PDMS micro channel with thin film sensors for thermal analysis of chemical reactions [13]

As discussed earlier enthalpy and temperature one of the most important properties for the investigation of chemical reaction. Calorimeter is often used to measure the reaction enthalpy, and many different calorimetric systems have been developed during the last decades. Initially it was very difficult to characterize exact enthalpy change at micro scale with classical calorimeter. So it is better to study such reaction on a small scale, thus involving only small amount of very reactive compound and keep the safety of the reaction at an early stage of development. There have been many methods developed to measure the temperature profiles at microscale. The thermocouple is cheap and simple, which is most extensively used in microreactors [14-15]. But it has to be embedded into the channel and it may affect the flow behavior in systems like EWOD and micro channels. Also, a thermocouple can only get one result at distinct points and also it affects the flow in a microsystem. Therefore, non-intrusive methods have been

suggested to get the reliable and accurate characterization of temperature sensors for micro devices. Temperature-dependent fluorescent dye was used to measure the temperature distribution at microscale [16] and also liquid crystals [3] have been used to measure temperature ranges at microscale. [17] Peltier elements and Zener diodes have been used for temperature measurement for microscale, but it provides non-local or noisy results. However, all these methods are usually sensitive to the reacting conditions and also it is not capable of measuring exact temperature. Not only that, the small measuring range also limits their application.

Even though many innovative methods such as Raman spectroscopy [18,19], infrared thermometry [20] and infrared camera [21] are used for temperature and heat flux sensing recently. These methods have an advantage of recording the complete and continuous temperature field of a specified area. Laser Raman spectroscopy was used to measure the in situ temperature of water in micro channels with better accuracy [19]. The procedure had a lateral local resolution of approximately 15 µL and a depth resolution of 25 µL. Peltier elements and Zener diodes have been tested for thermal measurement, but provide non-local or noisy results. Enthalpy of fast exothermal reaction of H_2SO_4 and NaOH with different molarities was measured with infrared thermography in a microreactor having coiled capillary [21]. A microsystem with infrared thermometry and the temperature profiles of the fast exothermal hydrolysis of tetraethoxysilane were measured inside microchannel at different flow rates [20]. It was [22] presented that thermal analysis of microfluids containing aluminum oxide nanoparticles in a microfluidic platform using an infrared camera, which gives the contact less, three dimensional with high resolution temperature sensing. However, there are two substantial conditions required for the infrared thermometry, which limit its wide applications. First is the microchannel must be covered with infrared transparent materials, such as silicon,

sapphire or germanium [23]. The second condition is that the system needs a cautiously calibration due to the radiation losses. An another important limitation is problem of visibility because this IR material are generally opaque in visibility, so we are not able to see what is going inside microchannel.

The primary goal of this research was to develop a temperature sensing EWOD platform which should capable of measuring small temperature for various chemical synthesis application. The main objective of this work was to provide a quick, safe and nonintrusive method to obtain the temperature profiles of an exothermic reactions with an ITO RTD [24,3] with is quite cheaper technique than other temperature monitoring technique. Before using ITO RTD it needs to calibrated to plot calibration curve in order to convert resistance change in to temperature change. The temperature profile of the reaction was intended to record which would then help to calculate the enthalpy of reaction. As there are much significant losses at microscale a Multiphysics numerical simulation was also needed to carry out to validate experimental model on COMSOL Multiphysics find out overall heat losses. The significance of overall heat loss estimation is that it is useful to estimate the process capability of EWOD microreactor for chemical synthesis which could be operated in a control atmospheric condition like low pressure, low velocity and high humidity atmosphere to suppress overall heat losses, so that ITO RTD can able to sense exact temperature of reaction. Compared with the traditional calorimeter, the microsystem chemical reactor can provide a quick, safe and non-intrusive method to obtain the temperature profiles of an exothermic reactions.

CHAPTER 3 EXPERIMENTAL SETUP

3.1 Experiment setup overview

The experimental setup was mainly composed of a multilayer EWOD micro droplet reactor (Electrowetting on dielectric) device having 200 nm Indium Tin Oxide RTD temperature sensor embedded in it. The busbar of this ITO RTD was connected to wire by soldering with copper strip and this copper strip which was again adhered to ITO busbar with the help of conductive silver epoxy. This ITO RTD was electrically connected to the Agilent Data acquisition unit by terminal connector for taking the readings of resistance change. 2 no T-type thermocouple was also connected to the Agilent Data Acquisition unit to sense the temperature of surrounding medium during calibration. For continuous measurement with respect to time LabVIEW programming was done which will be explain in later section. As soon as the LabVIEW program is turn on the Data Acquisition system will start taking the 4 wire resistance readings for ITO RTD temperature sensor.

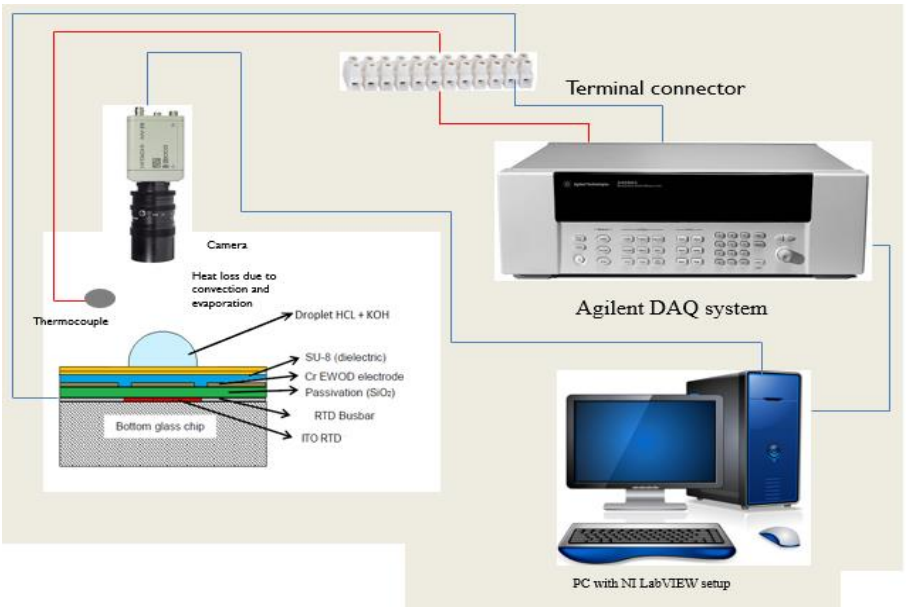

Figure 3-1 Experiment setup block diagram

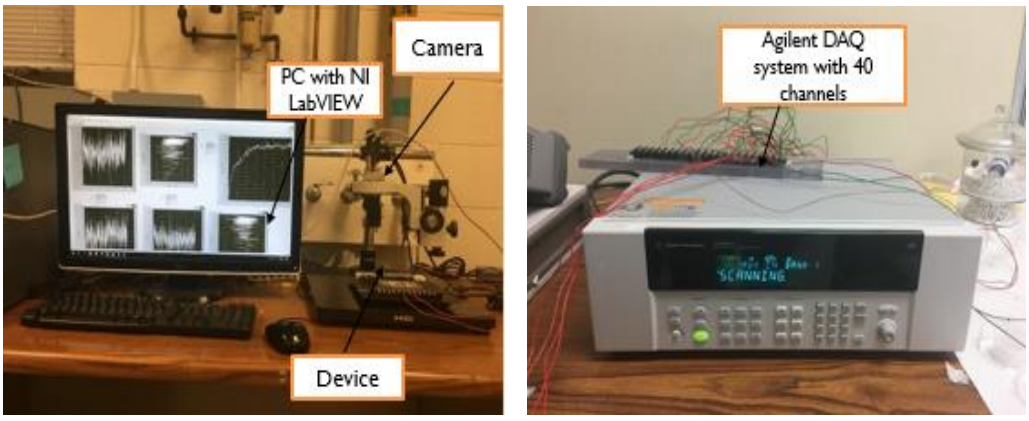

Figure 3-2 Actual Experiment setup

3.2 Mask Design

The mask for photolithography process for heater, EWOD electrodes fabrication was designed using L-Edit software by Tanner EDA [25]. The final circuit design was exported to GDS (Graphic Data System) file type and was then converted to PostScript (PS) format using LinkCAD software [25]. The PS format helps us to view the final design which was similar to PDF format. This PostScript file was sent to a mask printing company, CAD/Art Services Inc., Oregon. For convenience in designing, the mask for SiO2 passivation layer patterning is done on SolidWorks. This mask is then printed on a fine transparency sheet with a printer. Five transparency sheets were printed and stacked together. The photolithography is explained in detail in upcoming section.

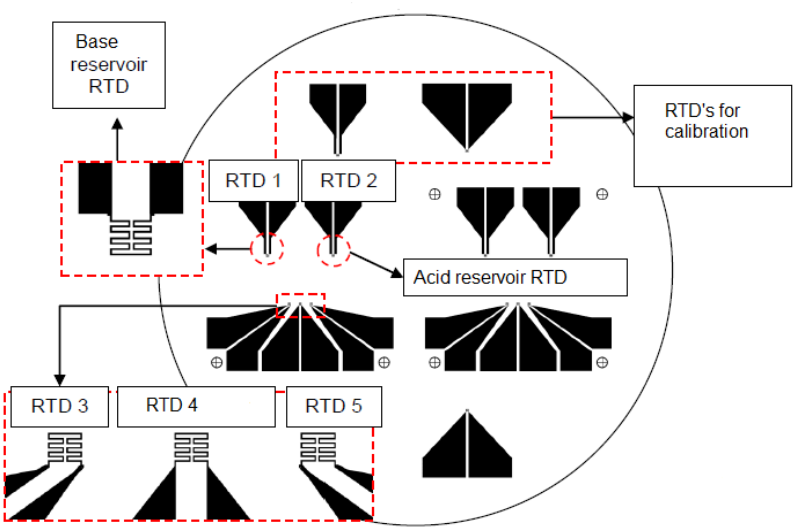

(a)

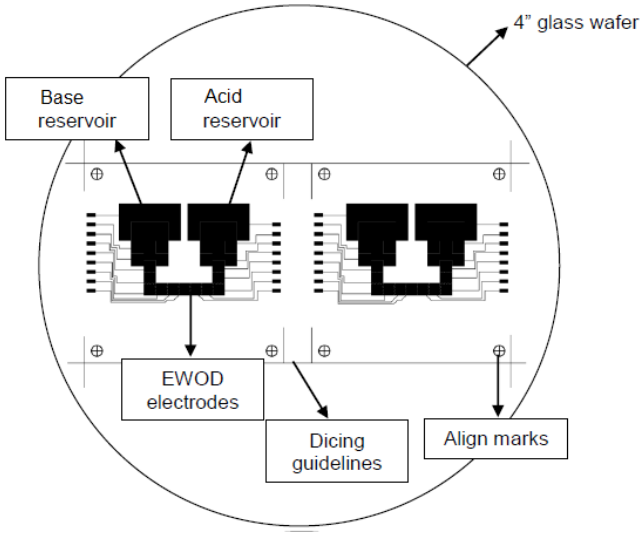

(b)

Figure 3-3 Photolithography Mask for PR patterning [3], (a) ITO RTD Mask, (b) Chromium EWOD electrode mask

3.3 Micro Droplet Reactor Device Fabrication

EWOD bottom and top chip fabrication is done at Shimadzu Institute of Research technologies, University of Texas at Arlington Micro Nano Fabrication lab using MEMS photolithography technique. Initially commercially available ITO wafer was cleaned with acetone, isopropyl alcohol, methanol and DI water, it is allowed to dehydrate at 150 ^{o}C for 5 minutes. As shown in Figure3-4 first spin coating of Hexamethyldisilazane (HMDS) on pre-coated ITO substrate was done at 3000 RPM for 30 seconds which was followed by the soft bake on hotplate at 150 ^{o}C. Next layer of photo resist, (S1813) was spin coated at 4000 RPM for 30 seconds.

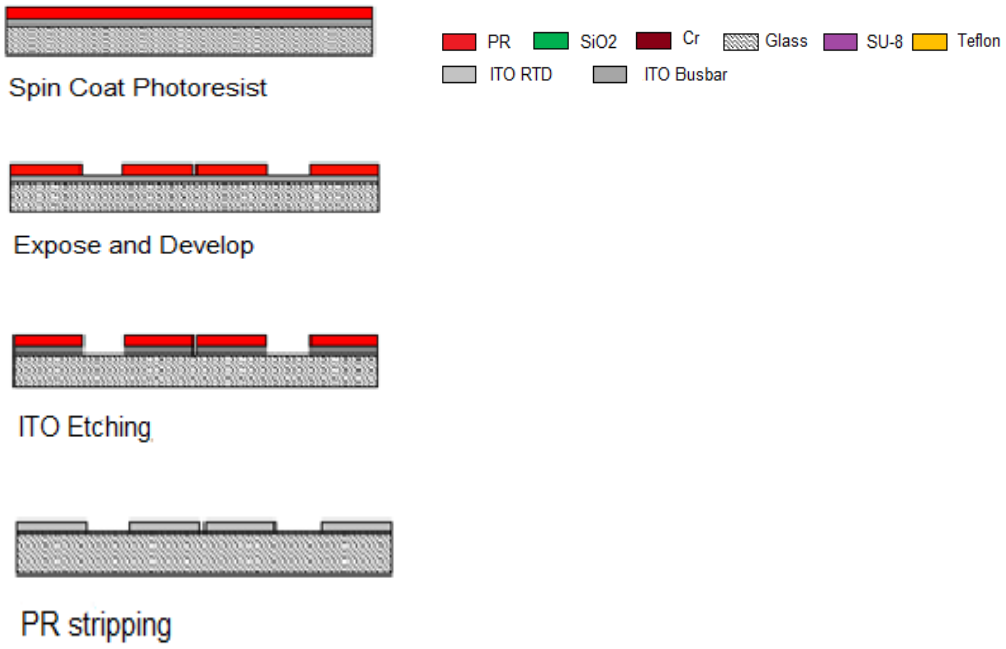

Figure 3-4 ITO RTD Fabrication

The wafer was soft baked at 115 ^{o}C for 1.5 minutes and then exposed to UV light for 8 seconds. Thereafter ITO substrate was subjected to post exposure bake at 110 ^{o}C for 1 minute and it was allowed to cool till room temperature, then it was completely immersed in a developer MF-319 solution and developed approximately 90 seconds till exposed PR dissolved in the developer solution leaving behind the pattern same as the layout mask during UV exposure, and resistance was checked with multimeter where the photoresist was not present.

The PR pattern was then checked in a microscope in order to make sure of any discontinuity. After proper inspection in a microscope PR patterned ITO wafer was allowed to hard bake on hot plate at 150 ^{o}C for 5 minutes for proper ITO etching. Next, the ITO etchant solution was prepared with ingredients HNO_3, HCL, DI water having volume ratio of 1:8:15 and it is allowed to heat at 55 ^{o}C on a hotplate. The PR patterned ITO wafer was slowly immersed in an ITO etchant solution and allowed to etch for 1.30 minutes. Etching was done till substrate shows zero resistance on substrate in a multimeter where ITO is not pattern, also the pattering of etched ITO heater was examined in a microscope. The substrate was dipped in a MF-1165 (PR stripper) solution for 6 minutes to remove the PR from patterned ITO heater. The resistance of ITO RTD was checked with multimeter which shows the resistance in the range of 1.2-1.5 k-ohm range.

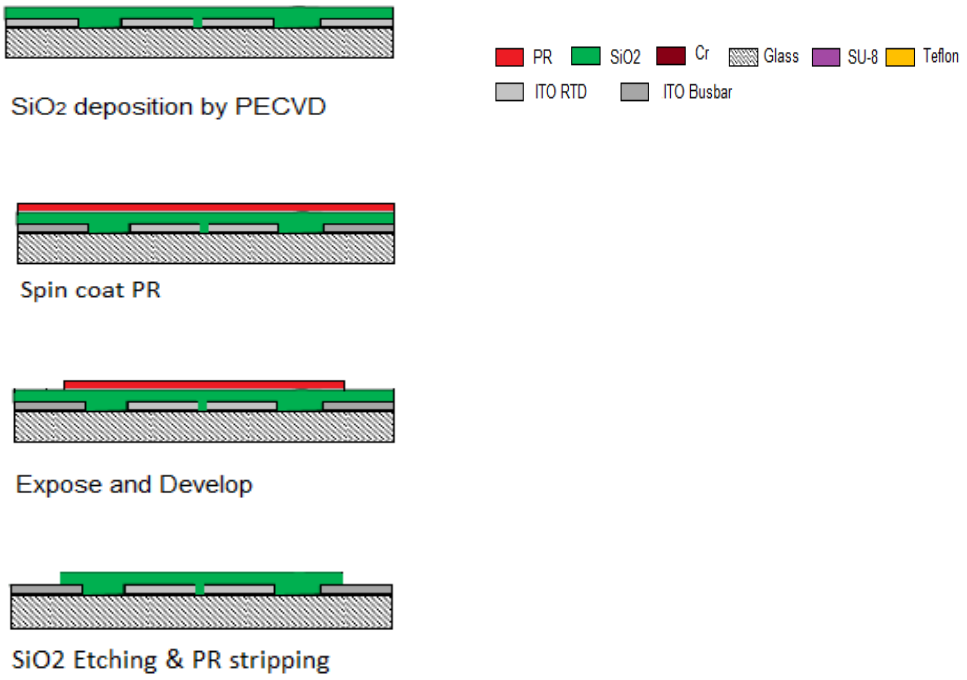

Figure 3-5 Passivation layer deposition

Now again the device was cleaned with acetone, isopropyl alcohol, methanol and DI water, it is allowed to dehydrate at 150 ^{o}C for 5 minutes. After dehydrating the substrate 100nm SiO2 passivation layer was coated with PECVD. Now the wafer was cleaned and allowed to dehydrate as done earlier and PR patterning on SiO_2 layer was done again with same recipe. On the mask the alignment marks were provided in order to align it with the patterned ITO RTD and new SiO_2 pattering mask before UV exposure. After patterning SiO_2 etching is done in Buffer oxide solution for 3 minutes and resistance was checked with multimeter. Etching was done till the multimeter shows resistance of ITO RTD followed by PR stripping for 6 minutes.

Again substrate was cleaned with acetone, isopropyl alcohol, methanol and DI water. It is again allowed to dehydrate at 150 ^{o}C for 5 minutes. Now 100nm chromium was deposited in Electron Beam Metal (E-beam) deposition followed by cleaning with isopropyl alcohol, methanol, DI water and dehydrate at 150 ^{o}C for 5 minutes.

Thereafter, again the PR patterning was done on the chromium layer with same recipe for EWOD electrodes patterning with different mask. Before UV exposure substrate was properly aligned with the mask, rest the PR patterning procedure was same as previous steps. After hard bake at 150 ^{o}C for 5 minutes, chromium etching was done for approximately 5-6 minutes. The continuity of all electrodes in a microscope was checked. After ensuring the continuity and PR patterning of chromium was done followed by PR stripping of hard bake PR in MF-1165 PR stripper solution and again continuity was checked with multimeter.

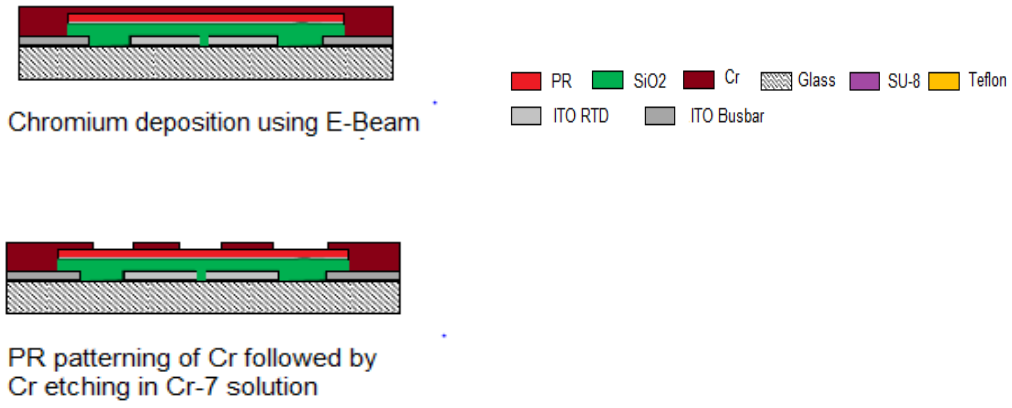

Figure 3-6 EWOD Cr layer deposition

Once the PR was stripped, a 5 µm thick negative photoresist SU-8 layer was spin coated at 3000 RPM, it was UV exposed for 7 seconds and developed to form the di-electric layer. Lastly, a thin layer of Teflon was spin coated at 3000 rpm in the end to form a hydrophobic layer on the layer of wafer.

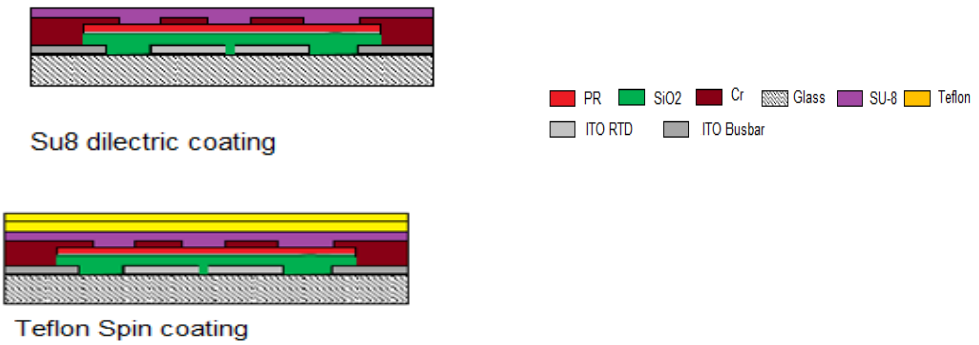

Figure 3-7 Su8 and Teflon layer spin coating

3.4 LabVIEW setup

The lab view programming was done for DAQ (data acquisition) Agilent 34980A for measuring temperature of oil bath with two J-type thermocouple. Also programming was done for 4-wire resistance to measure 4 wire resistance of an ITO RTD. In order to take continuous reading of two J-type thermocouple and 4 wire resistance with respect to real time, a time loop was used as shown in Figure 3-5. In this LabVIEW setup 4-wire wire resistance method was used to take the readings of ITO RTD which is more accurate than 2 wire resistance.

First and foremost, VISA resource name was selected from the front panel, then from instrument I/O library given Agilent 34980A driver was selected and initialize block

was selected to initialize the program. Thereafter, thermocouple configure VI and 4 wire resistance configure VI were inserted. In thermocouple configure VI reference temperature, type of thermocouple and channel list is specified out of all 40 channels. Again for 4 wire resistance VI channel list was specified. Now scan VI for both thermocouple and 4 wire resistance was selected from instrument I/O from configure list and channel list was selected as shown in Figure 3-8. 4 wire resistance measure and thermocouple measure VI is selected from the list and it is placed under “while time loop” as shown in Figure 3-8. Here time step for time loop is 100 msec. Here all the values of temperature as well as resistance were stored in an array. In a given figure 3-5, it can be seen that various graphs were plotted like resistance v/s time, thermocouple temperature v/s time and average temperature v/s resistance over a period of time using different VI.

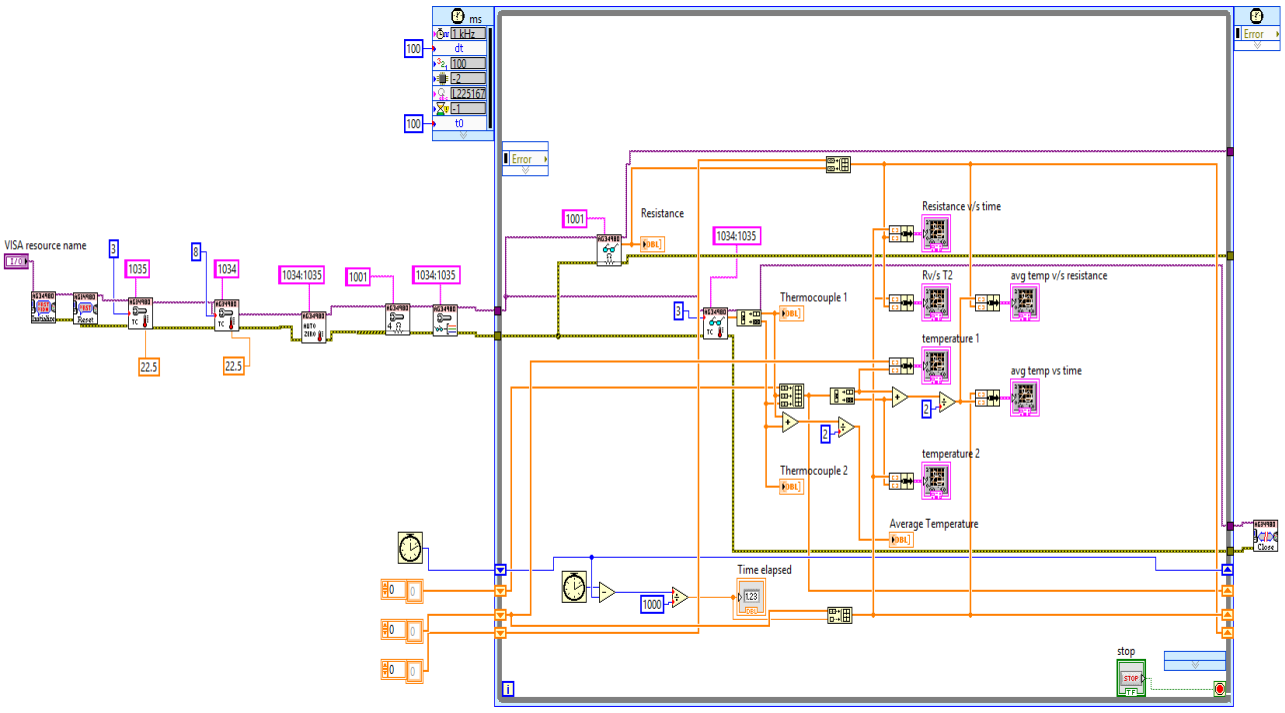

Figure 3-8 LabVIEW program

3.5 Indium Tin Oxide RTD calibration

The resistance versus temperature relationship is describe as the amount of resistance change of the sensor per degree of temperature change. The relative change in resistance (temperature coefficient of resistance) varies only slightly over the useful range of the sensor or a given metal. Metals such as platinum, nickel and copper are generally use as a resistance temperature detector because of their repeatable resistance versus temperature relationship and their operating range of temperature of temperature. Most commonly platinum [26] is used a RTD as it is having the superior properties for resistance temperature detector compare to other metals. Platinum is having high temperature range of around -272 ^{o}C - 961^{o}C to which makes it versatile for temperature detection in all condition.

In MEMS fabrication thin film elements are deposited which have a coil resistance sensor on a glass substrate. In this research indium tin oxide semiconductor was used as a resistance temperature detector because it is quite cheaper than platinum and moreover commercially available ITO wafers can be further patterned with photolithography MEMS fabrication process to get a desired pattern on it. In this research small temperature range was low so, Indium tin oxide was suitable, not only that in small temperature ranges Indium Tin oxide temperature versus resistance cure is repeatable and it is quite sensitive to small temperature change. The desired operating range was found to be 0 ^{o}C to 120 ^{o}C approximately in which ITO is having linear Resistance versus temperature characteristics [3].

The calibration of ITO RTD was carried out to determine the value of temperature coefficient of resistance (α) with the help of resistance and temperature values. Before carrying out the calibration process the base resistance of an ITO RTD was measured at an atmospheric temperature. Then a copper strip was adhered to the

ITO heater busbar with the help of conductive silver epoxy adhesive and it was kept in an over at 75 ^{o}C for 2 hours, it was then allowed to cool at room temperature for 10 minutes. Now two wires were soldered to the copper strip on ITO busbar. Two terminals from the busbar were connected to data acquisition (DAQ) system hardware which is been control by LabVIEW program as shown in Figure 3-9. DAQ system is capable of measuring resistance to RTD at a regular time frame and with the help of LabVIEW program this measured resistance data can be stored in system and can be plot with respect to time using inbuilt VI.

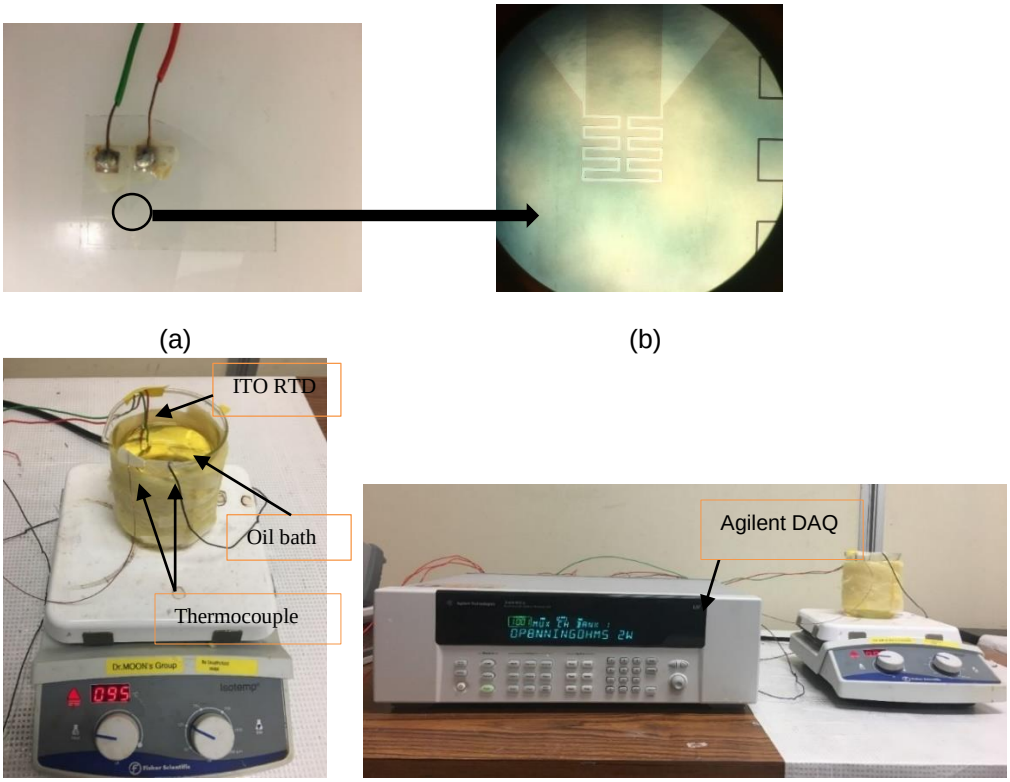

(a) (b)

(c) (b)

Figure 3-9 (a) ITO RTD for calibration, (b) Magnified view, (c) Hot plate with oil bath, (d) Calibration setup

As shown in above Figure 3-9 the ITO RTD on which the wire was bonded and soldered was dipped in a beaker full of engine oil. The beaker is kept on a hot plate which maintains constant temperature on its surface. Magnetic stirrer was also placed in an oil to maintaining uniformity of temperature in an oil by continuously stirring it at constant rpm. Three T-type thermocouple were used to sense the temperature of oil bath. Slowly and gradually the temperature of a hot plate was increased and resistance reading was monitored at regular temperature intervals. The reading of resistance was taken when all the three thermocouple shows nearly same temperature. Reading of the resistance was taken till the temperature of oil bath went up to 100 ^{o}C. When it reaches to 100 ^{o}C again slowly the temperature of hotplate was reduced and the readings was taken. The cycle was repeated and it followed the same curve. After the resistance versus temperature data was plotted temperature coefficient of resistance (α) was calculated with the given formula.

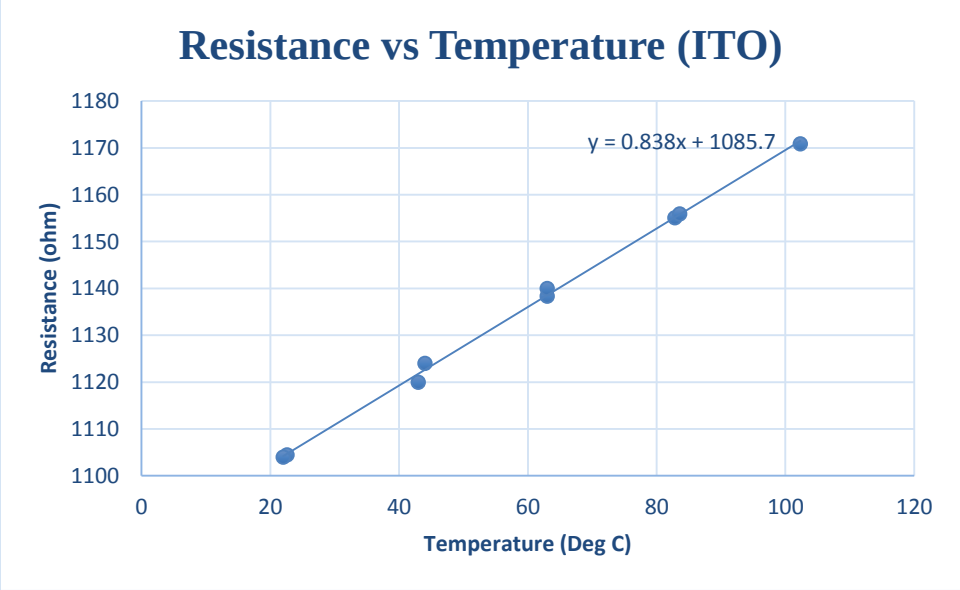

Figure 3-10 Calibration curve of ITO RTD

$R=R_0[1+\alpha(T-T_0)]$

Where,

R= resistance at temperature T.

R_0 = Base resistance at atmospheric temperature T_0 =1104.5 ohm.

α = Temperature coefficient of resistance = 0.0007 (1/ ^oC).

T_0 = Base temperature 22.2 ^oC.

With the help of above equation, the value of temperature coefficient of resistance (α) was calculated and ultimately by measuring the value of resistance in an experiment it was again converted back into the temperature change with the help of above calibration equation.

3.6 Solution Preparation

3.6.1 2 Molar NaOH aqueous solution from NaOH Flakes

To prepare 1 Molar solution of NaOH, approximately 40 grams of NaOH flakes (Molecular weight of NaOH is 39.997 gm/mole) was dissolved in 1 litre of DI water and it is stirred till the solution completely dissolves in it and it makes an aqueous solution. With respect to above proportion 1.25 grams of NaOH is dissolve in 31.25 ml of DI water to make 1 Molar aqueous solution of NaOH.

3.6.2 2 Molar KOH aqueous solution from KOH flakes

For 1 KOH flakes preparation approximately 56 grams of KOH (Molecular weight of KOH is 56.10 gm/mol) was taken and dissolved in 1 liter of DI water, solution was stirred until all the particles of KOH was well dissolved in DI water. With respect to this proportion 2 M KOH aqueous solution was prepared, so for that we need to dissolve 112

grams of KOH flakes into 1 litre of DI water solution. By scaling down we can dissolve 11.2 gm of KOH flakes into 100 ml of DI water to prepare a sample of 2 M KOH aqueous solution.

3.6.3 2M HCL from concentrated HCL

To make 1.0L of this solution.

This will have mass = 1180gram - from the density

Mass of HCl = 36/ (100*1180) = 424.8 gm HCl

To calculate number of moles of HCl = 424.8/36.45 = 11.65 mol in 1000 ml of solution

Here we want to make 500mL of 2.0M solution

Use of dilution equation

$M_1 V_1 = M_2 V_2$

$2.0 \times 500 = 11.65 \times V_2$

$V_2 = (2.0 \times 500)/11.65$

$V_2 = 85.8$ mL

Measure out 85.8mL of the concentrated HCL and dilute to total 500mL.

3.6 Experimental Procedure

The experiment was performed at an open atmospheric room temperature and pressure. As shown in Figure 3-11 shows the micro droplet reactor device having embedded ITO RTD in it. Since this micro droplet reactor device is an EWOD device so it was required to have volume equal to the volume of one electrode so carry out experiment with sessile droplet without EWOD motion. The volume of droplet can be calculated as follows

Volume of droplet = area of electrode x height of spacer

$= 2.5 \times 2.5 \times 0.18\ (mm^3) = 1.125\ mm^3 = 1.125\ \mu L$

The reason behind taking 1.125 µL amount of volume is that in an experiment with EWOD motion after pinching a droplet from reservoir approximately 1.125 µL of volume of droplet most likely to be pinched off with spacer gap of 180 microns.

As shown earlier in Figure 3-9 the ITO busbar terminals were soldered with a wire which was again connected to DAQ multiplexer channel. Now in this experiment it was required to monitor resistance change of RTD with respect to time so, for that existing calibration LabVIEW program was used. As we knew that calibration LabVIEW program was setup for 2 thermocouples and 1 RTD measurement. So, in that case same LabVIEW program was used in which thermocouple was used to measure the temperature of solution before mixing which was 21.6 ^{o}C and 4 wire resistance measurement of RTD was used for monitoring temperature in a form of resistance change of micro droplet after mixing.

As shown in Figure 3-11, a micro droplet of 1.125 µL of each 2 M HCL and 2M KOH was dispensed on an electrode having ITO RTD embedded in it at the same time with pipette. Since this reaction is an exothermic reaction there will be a rise in temperature of ITO RTD with respect to time.

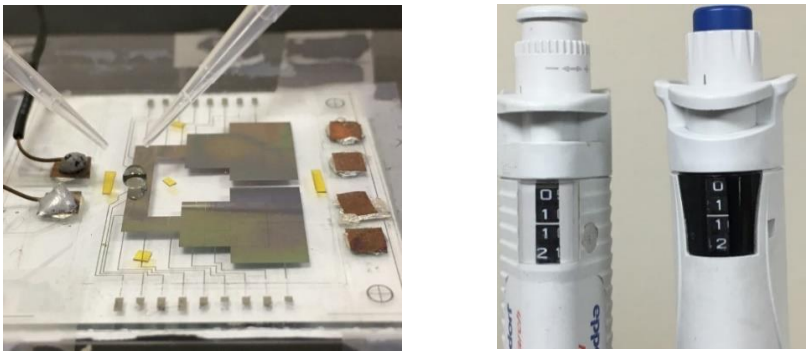

(a) (b)

Figure 3-11 (a) Actual Micro Droplet reactor with droplet of acid and base, (b) Fixed volume Pipette

The experiments were carried out at room temperature (22.2 ^{o}C) with a micro droplet of both reactants having exact volume 1.12 µL each. The Data Acquisition system was controlled through NI LabVIEW program to take RTD readings. First the LabVIEW program was allowed to run for around 400 seconds till it shows the steady atmospheric temperature. When the program shows steady atmospheric temperature then 1.125 µ-lit droplet of 2M HCL and 2M NaOH was dispensed carefully with fixed volume pipette at the same time on the EWOD electrode having ITO RTD embedded in it. Data acquisition then began and temperatures were recorded by embedded thin film ITO RTD temperature sensors. The reaction of 2M HCL and 2M NaOH is fast and exothermic, and therefore the extent of reaction and the heat released are limited by the mixing of reactants, which is carried out essentially by molecular diffusion. As soon as the 1.12 µL droplet of acid and base were dispended the temperature started to rise. The maximum temperature rise was observed 2.0 ^{o}C and also it depends on atmospheric conditions. Once this maximum was reached, the temperature longitudinal profile tends to decrease due to heat conduction through the glass substrate, convection in an atmosphere. Along with conduction and convection there was one more mode of heat transfer which was investigated later, the evaporation due to diffusion of water particles into the atmosphere which was responsible for further decrease in temperature below the atmospheric temperature.

CHAPTER 4 THEORETICAL CALCULATIONS

4.1 Reaction 1

The following neutralization reaction of 2 Molar solution of Sodium Hydroxide which is strong base and 2 Molar solution of Hydrochloric acid (strong acid) was mixed to form aqueous solution of Sodium chloride and water, which is an endothermic reaction.

$$NaOH_{(aq)} + HCl_{(aq)} \rightarrow NaCl_{(aq)} + H_2O_{(l)} + Q$$

4.1.1 Enthalpy change

Enthalpy of reaction per mole= [Enthalpy of formation of products] – [Enthalpy of formation of reactants]

$\Delta H_{reaction} = [\Delta H_f(H2O_{(l)}) + \Delta H_f(NaCl_{(aq)})] - [\Delta H_f(HCl_{(aq)}) + \Delta H_f(NaOH_{(aq)})]$

$=[1(-285.83) + 1(-407.25)] - [1(-167.15) + 1(-470.09)]$

$= -55.84$ kJ/mol

Q= -55.84 kJ/mol (exothermic reaction)

4.1.2 Entropy Change

$\Delta S_{reaction} = [\Delta S_f(H2O_{(l)}) + \Delta S_f(NaCl_{(aq)})] - [\Delta S_f(HCl_{(aq)}) + \Delta S_f(NaOH_{(aq)})]$

$\Delta S_{reaction} =[1(69.91) + 1(115.48)] - [1(56.48) + 1(48.25)] = 80.66$ J/K

$\Delta S_{reaction} = 80.66$ J/K-mol (increase in entropy).

4.1.3 Gibbs Free Energy of Reaction

Gibbs Free Energy of Reaction = [Gibbs free energy of formation of products] - [Gibbs free energy of formation of products]

$\Delta Gf°_{reaction} = [\Delta G_f(H2O_{(l)}) + \Delta G_f(NaCl_{(aq)})] - [\Delta G_f(HCl_{(aq)}) + \Delta G_f(NaOH_{(aq)})]$

$= [1(-237.18) + 1(-393.15)] - [1(-131.25) + 1(-419.18)] = -79.9$ kJ

$\Delta Gf°_{reaction} = -79.90$ kJ (spontaneous reaction)

For 2 M solution of each 1.125 µ-lit of NaOH and HCl we have equal no of moles. So, here we have 2.25 x 10^{-6} moles of both NaOH and HCL for each 1.125 µ-lit of 2 M solution

Q= -55.84 kJ/mol = ΔH

Q= -55.84 x no of moles (KJ)

= -55.84 x 2.25 x 10^{-6} x 10^{3} J

= 0.12564 J

$0.12564 = (m_a + m_b) \times c_g \times (T_f - T_i)$

$0.06282 = (0.0011+0.0011) \times 4.184 \times 10^{-3} \times 10^{3} \times \Delta T$

ΔT= 13.52 ^{o}C (Theoretical temperature rise).

4.1 Reaction 2

Again neutralization reaction of 2 Molar solution of Potassium Hydroxide which is strong base and 2 Molar solution of Hydrochloric acid (strong acid) was mixed to form aqueous solution of Potassium chloride and water, which is an exothermic reaction.

$$KOH_{(aq)} + HCl_{(aq)} \rightarrow KCl_{(aq)} + H_2O_{(l)} + Q$$

4.1.1 Enthalpy change

$\Delta H_{reaction} = [\Delta H_f(KCl_{(aq)}) + \Delta H_f(H2O_{(\ell)})] - [\Delta H_f(HCl_{(aq)}) + \Delta H_f(KOH_{(aq)})]$

$\Delta H_{reaction} = [(-419.55) + (-285.83)] - [(-167.15) + (-482.39)] = -55.84$ kJ/mol

$Q = \Delta H_{reaction} = -55.84$ kJ/mol (exothermic reaction)

4.1.2 Entropy change

$\Delta S_{reaction} = [\Delta S_f(KCl_{(aq)}) + \Delta S_f(H2O_{(\ell)})] - [\Delta S_f(HCl_{(aq)}) + \Delta S_f(KOH_{(aq)})]$

$\Delta S_{reaction} = [1(158.98) + 1(69.91)] - [1(56.48) + 1(91.75)]$

$\Delta S_{reaction} = 80.66$ J/K mol (increase in entropy)

4.1.3 Free energy changes of reaction

Gibbs Free Energy of Reaction (at 295 K) = [Gibbs free energy of formation of products] - [Gibbs free energy of formation of products]

$\Delta Gf°_{reaction} = [\Delta G_f(KCl_{(aq)}) + \Delta G_f(H2O_{(\ell)})] - [\Delta G_f(HCl_{(aq)}) + \Delta G_f(KOH_{(aq)})]$

$\Delta Gf°_{reaction} = [(-414.55) + (-237.18)] - [(-131.25) + (-440.58)] = -79.9$ kJ/mol

$\Delta Gf°_{reaction} = -79.90$ kJ/mol (spontaneous)

From, $\Delta G = \Delta H - T\Delta S$

$= -55839.99 - (293 \times (80.66))$

$= -79.89$ kJ/mol (spontaneous reaction)

Now, $\Delta H_{reaction} = Q = -55.84$ kJ/mol

$Q = -55.84 \times$ no of moles (KJ)

$= -55.84 \times 2.25 \times 10^{-6} \times 10^{3}$ J

$= 0.12564$ J

Again, $0.12564 = (m_a + m_b) \times c_p \times (T_f - T_i)$

$0.06282 = (0.0011+0.0011) \times 4.184 \times \Delta T$

$\Delta T = 13.52\ ^oC$ (Theoretical temperature rise)

CHAPTER 5 NUMERICAL STUDY

5.1 Introduction

For validation of experimental data, a numerical simulation was carried out on commercial simulation software called COMSOL Multiphysics. COMSOL Multiphysics is a very powerful tool which uses finite element analysis solver. The finite element method (FEM) is a numerical technique for finding approximate solutions with respect to boundary value and initial value problems for partial differential equations. It subdivides a large problem into smaller and simpler parts like rectangular or triangular that are called finite elements and this process it is also called discretization. These finite elements form the interconnected network of the concentrated nodes. It using the predefined equations of solver to calculate values at every node. Rather than solving whole problem of entire geometry in entire one operation, each and every node of the network is analyzed and their results are synthesized to get the complete analysis of the geometry. The interrelating values of all the nodes gives the behavior of the whole geometry [27].

5.2 Problem Definition

From an experimental data shown previously it was known that there was a certain amount of temperature decrease in a droplet below the room temperature due to evaporation of droplet itself because of the diffusion of water particles into the flowing air. So in this problem we were having total three modes of heat transfer conduction through bottom chip, convection through air and most important evaporative cooling which is a transient heat transfer problem. So to incorporate evaporative cooling as well as conduction and convection in our model we need three physics that is fluid flow, heat transfer and transport of diluted species [28]. The first step was to compute the laminar

flow field out stationary time independent simulation with normal fluid dynamics mesh. After that, the resulting velocity field will be used to compute the transport properties of heat and moisture which is time dependent study whose time range was taken as 0-100 seconds.

5.3 Defining parameters

For simulation 2 important assumptions were made. The first assumption is that reaction is homogenous, reaction time is very fast, 12.5 seconds and reaction will complete after 12.5 seconds. So in this simulation model, a time dependent function Qgen was defined, which depend on volumetric heat flux (q) whose value was defined till 1 to 12.5 seconds and after 12.5 seconds its value was 0. In our model time range of 0-100 seconds was considered. Again volumetric heat flux (q) was defined in a global parameters section whose value was calculated from theoretical calculations for enthalpy of reaction for given reaction, total reaction time, final volume after mixing and it was coming out to be 4.467 x 10^{-3} W/mm^3. The another global parameters M_w, H_vap, rel_hum, rho_w_max are molar mass of water, heat of evaporation, relative humidity and maximum amount of water in fully saturated air at 22 ^oC temperature respectively. From all the above values inlet air concentration c0 which was defined as c0= (rel_hum x rho_w_max)/ M_w.

Parameters

Name	Expression	Value	Description
q	4.46e-3 [W/mm^3]	4.46E6 W/m^3	
H_vap	2454[kJ/kg]*M_w	44209 J/mol	Heat of vaporization
c0	rel_hum*rho_w_max/M_w	0.57286 mol/m^3	Inlet concentration
rho_w_max	0.0172[kg/m^3]	0.0172 kg/m^3	Maximum amount of water for 100% humidity at 22°C
M_w	18.015[g/mol]	0.018015 kg/mol	Molar mass of water
rel_hum	0.6	0.6	Relative humidity

Table 5-1 Parameters defined for Numerical Simulation

Data source: Local table

Function name: Qgen

t	f(t)
0	0
1	q
10	q
12.5	q
13	0
25	0
100	0

Table 5-2 Transient heat function Qgen

5.4 Geometry Modelling

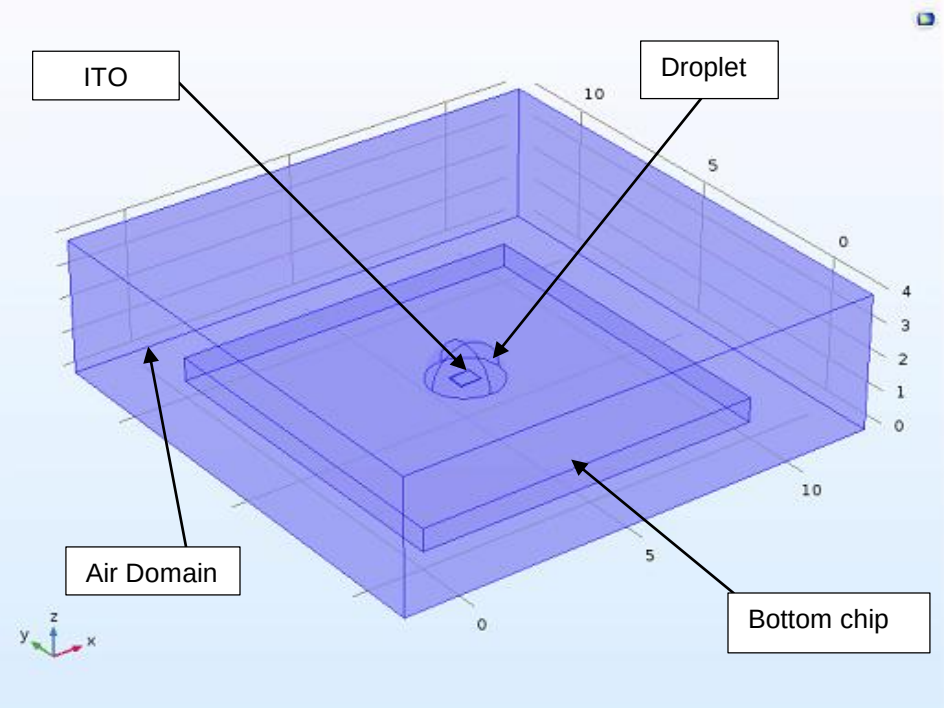

(a)

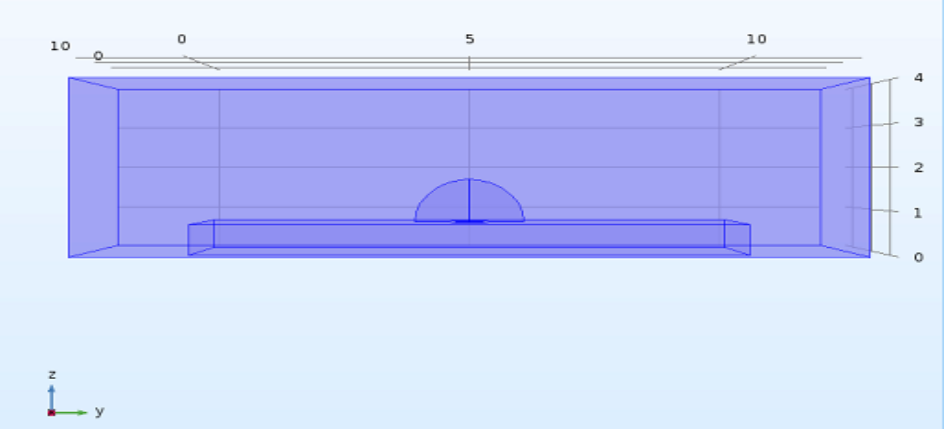

(b)

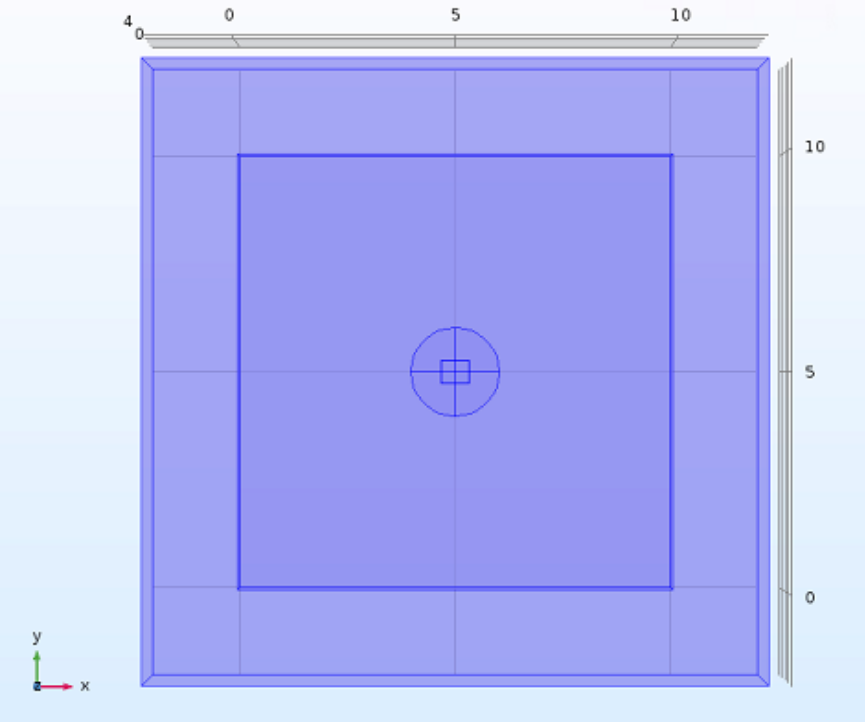

(c)

Figure 5-1 (a) 3D view of geometry, (b) side view of the sessile droplet, (c) Top view of the sessile droplet

Part name	Length (mm)	Breadth (mm)	Height (mm)
Bottom chip	10	10	0.7
Air Domain	14	14	4
ITO RTD	0.62	0.52	0.02

Drop	Diameter (mm)
	1.024

Table 5-3 Dimension of CAD model

The shown dimensions are the scaled dimensions of bottom chip and air domain. The reason behind scaling the dimension is to avoid the problem of divergence of solution because of much difference in dimension of droplet and bottom chip.

5.5 Governing equations

In this model there were three modes of heat transfer conduction, convection and evaporation, so it is a Multiphysics problem. Hence Fluid flow, Heat transfer in fluids and transport of dilute species were chosen for study. In fluid flow interface an incompressible laminar flow with very low velocity was considered. In heat transfer in fluids interface droplet as a heat source and heat flow in all domains was considered. For transport of dilute species, boundary heat source was assigned on droplet surface and surface concentration as a boundary condition have been defined. In this simulation the droplet was considered to be saturated and with respect to that saturation boundary conditions were applied.

For fluid flow, an incompressible, time independent Naiver-Stokes equation was used.

$$\rho(u.\nabla)\, u = \nabla.[-pI + \mu\,(u.\nabla)^T] + F$$

$$\rho\nabla(u) = 0$$

For Heat transfer in fluids, time dependent Energy equation was used

$$\rho C_p \frac{\partial C_i}{\partial t} + \rho C_p\, u\, \nabla T + \nabla.\, q = Q + Q_p + Q_{vd} \quad , Q = -k\, \nabla T$$

For transport of dilute species, time dependent mass diffusion equation was used

$$\frac{\partial C_i}{\partial t} + \nabla.\, (-D_i\, \nabla C_i) + u.\nabla\, C_i = R_i$$

$$N_i = -D_i \nabla C_i + u\, C_i$$

5.6 Defining property of materials

After modeling the geometry, materials are assigned to each domain. In COMSOL Multiphysics there is a building materials library from which the materials are assigned to their corresponding domain. Here the droplet was considered as water because the concentration of acid and base was low and the product of this chemical reaction was salt and water. Again air and silica glass was assigned as a material to outer air domain and bottom chip respectively. Now most important was to define property of RTD material, as the ITO was present in the COMSOL Multiphysics building materials library, so it was required to defined its properties. The properties such as density, heat capacity and thermal conductivity were defined.

5.7 Fluid Flow interface

In this model flow of air to be single phase laminar flow with no turbulence for convective heat transfer is consider. First the simulation of fluid flow physics was done alone to determine velocity and pressure distribution, and this values were further used in heat transfer in fluid and transport of diluted species physics.

5.7.1 Initial condition

For fluid flow we have only domain 1, that is air domain was considered for the simulation. Initially temperature of air was taken 295 K, and also initial velocity and pressure was taken into account as 0 m/s and 0 Pa respectively.

5.7.2 Boundary condition

For fluid flow domain, no slip boundary condition was provided on the bottom plate with respect to air. Here in this model we have taken air inlet from boundary 4 and boundary 1,2,5 and 23 is consider as shown in Figure 5-2, with open boundary with normal stress equal to 0.

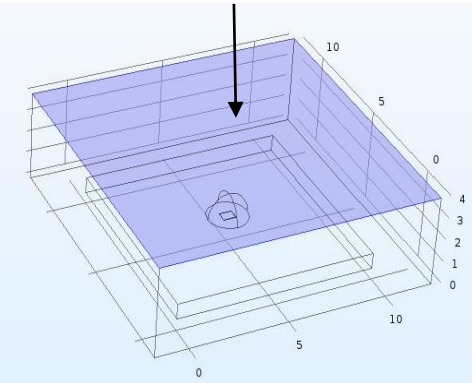

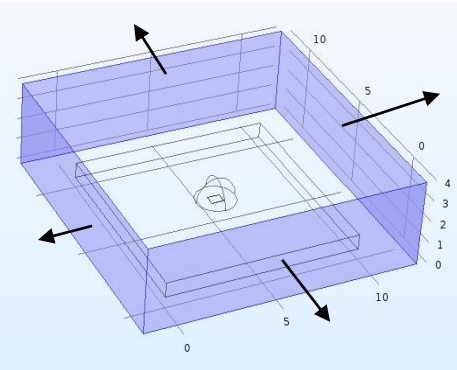

Inlet with U_0 = 0.001m/s, u = $-U_0$ n

Open boundary $[-pI + \mu (\nabla u + (u.\nabla)^T] n = f_0$ n

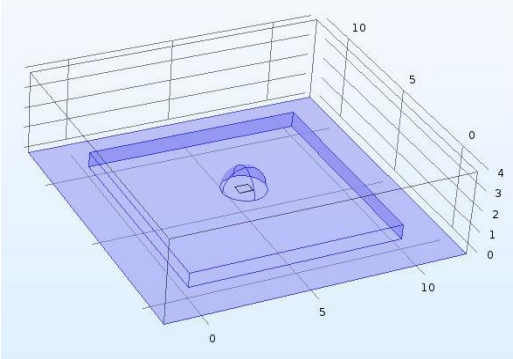

No slip boundary condition, u=0

Figure 5-2 Fluid flow boundary conditions

5.8 Heat transfer in fluids interface

For heat transfer interface in this model conduction, convection through air flow and evaporative cooling of droplet due to vapor pressure difference of droplet and inlet air. The evaporative cooling mainly happens due to diffusion of water particles into the inlet air. Here in this model for evaporation of droplet, droplet was considered to be fully saturated and according to that boundary conditions were applied.

5.8.1 Initial condition

Initially inlet air was considered at an atmospheric temperature and pressure that is, 295 K and 1 atmosphere respectively. Also droplet was considered to be stationary throughout the entire simulation and initial temperature and pressure was also taken same as 295 K and 1 atm.

5.8.2 Boundary conditions

Here conduction through bottom chip and ITO RTD was taken into account. Also convection through inlet air with 0.001 m/s velocity was considered. Here droplet itself

was considered as a heat source whose volumetric heat flux value lasted for 12.5 sec which was assumed to be the reaction time for experiment. So in heat source function Qgen(t) was used which was already defined earlier. Moreover, the boundary heat source was treated as fully saturated which can be shown in given Figure 5-3 and equation. Here fluid 2 was chosen as an air in which fluid type was taken as moist air whose concentration was already defined.

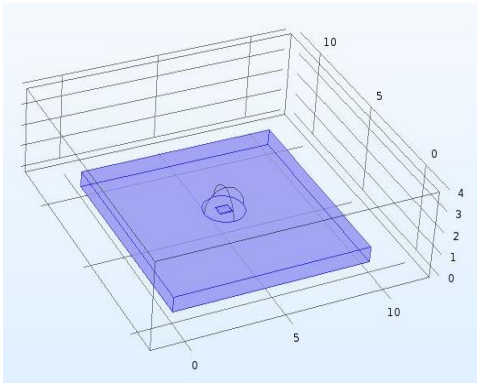

B.C for conduction in bottom chip and RTD

$\rho C_p u \nabla T + \nabla . q = Q$, $Q = - k \nabla T$

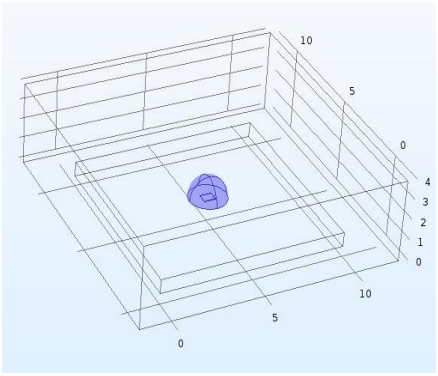

Transient Heat source Qgen(t), $Q = Q_0$

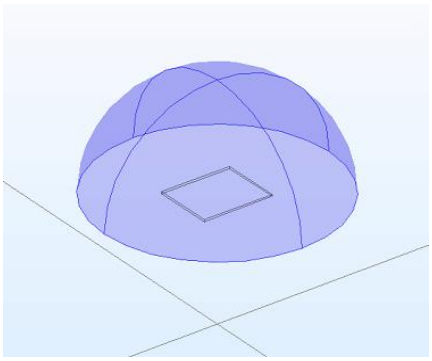

Boundary heat source, $- n.q = Q_b$

Saturated B.C: $-H\_vap*c\_lm[mol/(s*m^2)]$

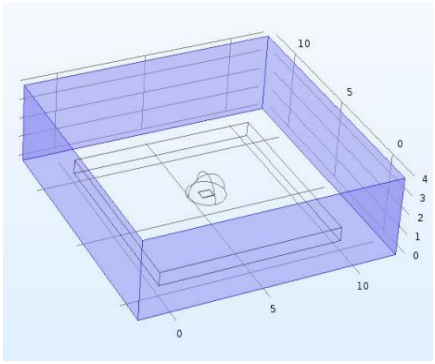

Open Boundary, $T=T_0$, if $n. u < 0$

$- n.q = 0$, if $n. u \geq 0$

Figure 5-3 Heat transfer in fluid B.C

5.9 Transport of Diluted species

In this transport of diluted species interface we have incorporate the diffusion of water particles into the flowing air, also as additional transport phenomenon convection was considered. For diffusion process to occur the primary requirement is to have concentration gradient, and also diffusion coefficient was defined.

5.9.1 Initial condition

First transport properties were assigned as an initial condition, for that air domain. Here diffusion process was taken as isotropic and diffusion coefficient was also assigned which is 2.6×10^{-5} m^2/s. Initial concentration of air was defined as c0 which was already calculated in global parameters.

5.9.2 Boundary condition

In this simulation the no flux condition was assigned on bottom boundary of the air and glass domain and also on vertical surface of bottom glass. Here the velocity field was directly taken from fluid flow interface. The droplet was considered to be completely saturated and saturated concentration boundary condition was applied for defining surface concentration. In surface concentration calculation saturated pressure was taken at an initial temperature of droplet. At the droplet surface the saturation concentration condition was applied at a saturation pressure, as shown in equation from Figure 5-4. With the moist air feature, the saturation pressure was calculated automatically and can be accessed directly.

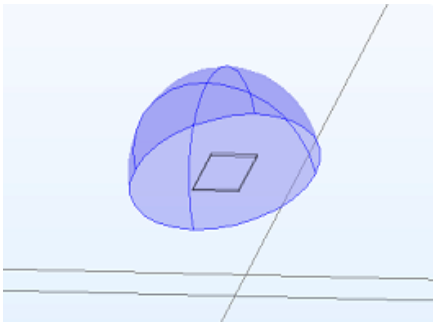

Concentration of droplet at saturated condition
c0 = Ht.psat/R_const*T (mol/m^3)

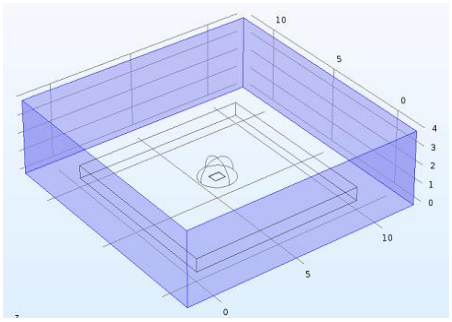

Outflow boundary condition
$-n.D_i \nabla C_i = 0$

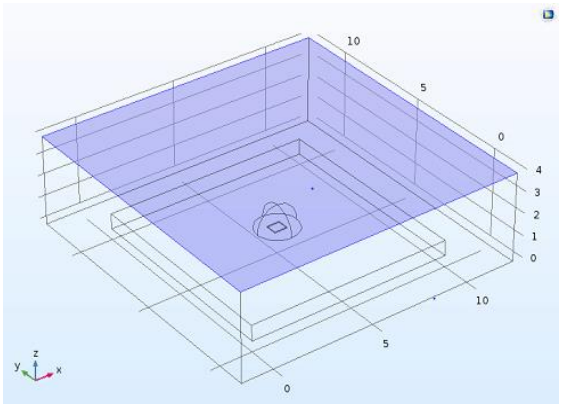

Initial Concentration c0= 0.57286 mol/m^3 (defined)

Figure 5-4 Transport of diluted species B.C

5.10 Multiphysics coupling

As mention earlier, there were 3 physics used in this model and all the three physics needs to be couple by some variables. In this model velocity of inlet air from fluid flow physics was used to couple it with heat transfer physics and transport of diluted species physics. In COMSOL Multiphysics there are predefined tools called flow coupling and non-isothermal which is used to couple all this physics. In flow coupling the source is

laminar flow and destination is flow and destination is transport of diluted species. In non- isothermal flow, specific density and temperature was used to couple it with other physics. The heat transfer in fluids and transport of diluted species equations was strongly coupled via the moist air feature using the concentration as input. This requires to configure a direct solver in a Fully Coupled approach.

5.11 Meshing

Initially for laminar fluid flow with no turbulence, stationary study 1 default physics control normal mesh was used. It is optimized for flow field calculations using a suitable mesh size and boundary layers according to the settings of the flow interface. In this model for study 2, time dependent study, user control free tetrahedral mesh of different sizes was used. As it was known that the dimension of the drop was quite small compare to bottom chip and air domain. For droplet and ITO RTD general physics extremely fine mesh was used as shown in Figure 5-5 since in final results we were intended to obtain the accurate surface average temperature of ITO RTD. Again for bottom chip general physics extra fine mesh and for air domain fluid dynamics normal mesh was used. Lastly adaptive mesh refinement was also used for proper mesh refinement in this model to get accurate results.

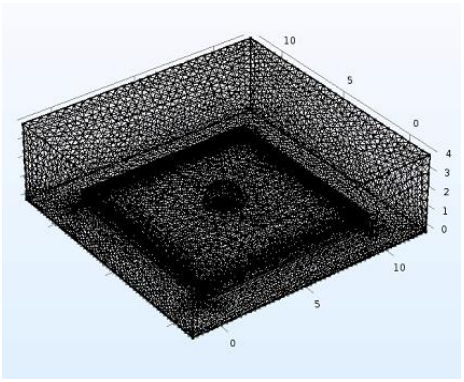

(a)

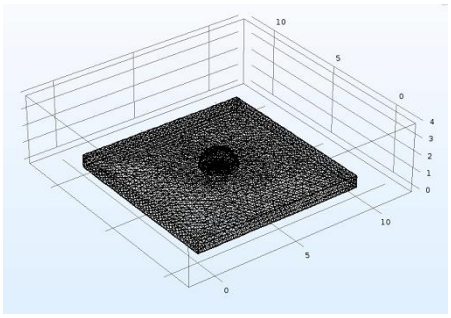

(b)

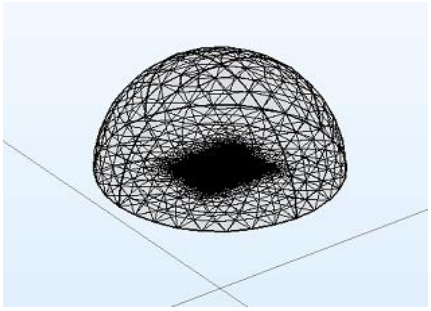

(c)

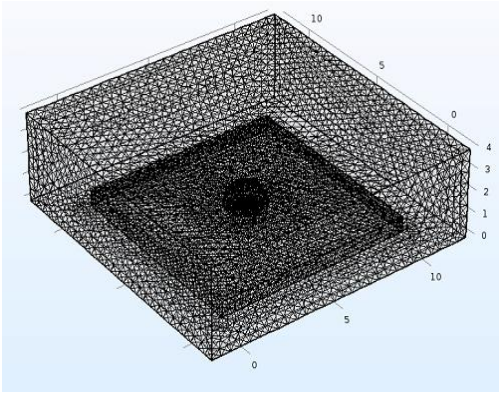

(d)

Figure 5-5 (a) physics control mesh for study 1, (b) Extra fine mesh for bottom chip, (c) extremely fine for mesh RTD and droplet, (d) fluid dynamics Normal mesh for air domain

5.12 Solution

5.12.1 Study 1 (stationary)

After meshing, in study 1, time independent solver the fluid flow model was computed to determine velocity field and pressure distribution which will be discuss further in detail in next chapter. This stored velocity and pressure values will be then useful to heat transfer and transport of diluted species to calculate heat transfer along with transport of water vapor.

5.12.2 Study 2 (Time dependent study)

In study 2, time dependent solver the values of temperature distribution of whole model with respect to time was computed, not only that concentration and relative humidity of whole domain was also calculated with respect to time for time range of 0-100 sec in which will be discuss further in an upcoming chapter.

5.13 Results plotting

Once the solution is computed, the results are plotted. For study 1, velocity and pressure profile were plotted along with streamlines. For study 2, surface average temperature of RTD, interfacial concentration of water droplet in air and volume average concentration of air domain was plotted

5.14 Roadmap

Figure 5-6 shows all the steps performed from starting to end for compute numerical solution.

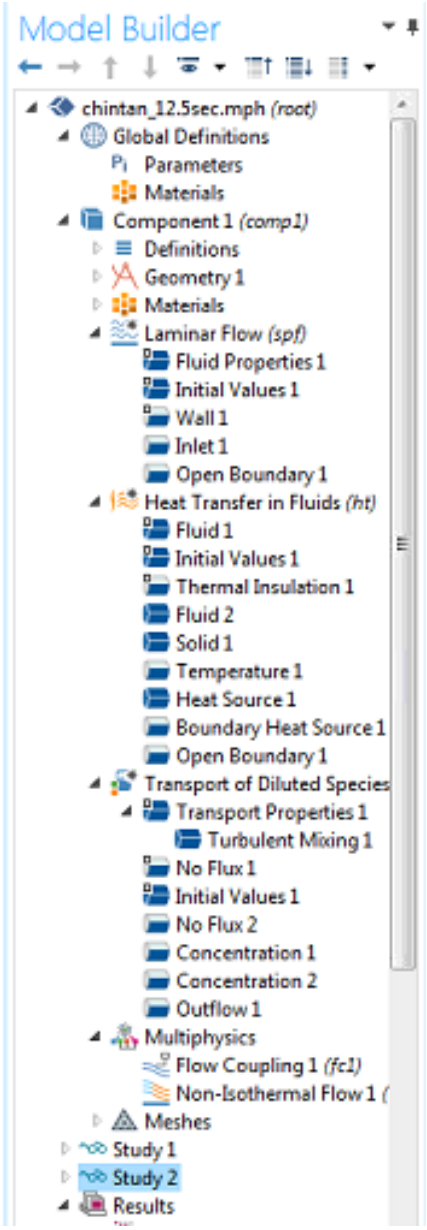

Figure 5-6 Roadmap

.

CHAPTER 6 RESULTS AND ANALYSIS

Initially the Data Acquisition is started and temperature of atmosphere was noted and when the DAQ shows the stable atmospheric temperature then with the help of fixed volume pipette, equal amount that is 1.125 µL of both acid and base were dispensed at same time on electrode. As soon as both the droplet of acid and base was dispensed on an RTD, the temperature started to rise as shown in Figure 6-1 due to exothermic nature of reaction.

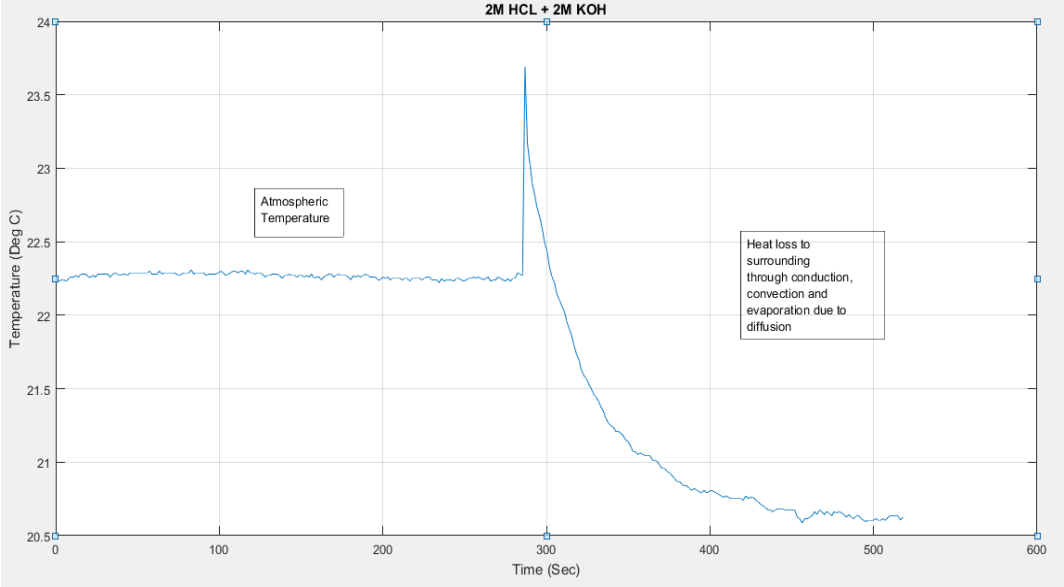

Figure 6-1 Experimental data of 2M HCl + 2M KOH

The Figure 6-1 shows the experimental data with 2M HCL and 2M KOH. As discussed earlier the readings of 4 wire resistance were taken at every 100 msec. As calculated in chapter 4 the theoretical temperature rise was 13.5 ^{o}C but due to high heat losses at microscale an ITO RTD can only able to sense only 2 ^{o}C maximum temperature rise of mixture.

Again 1.125 µL of each 2M HCL and 2M NaOH was dispensed on the electrode with a pipette. Since it's an exothermic reaction so it can be seen as a rise in temperature of ITO RTD as shown in Figure 6-1.

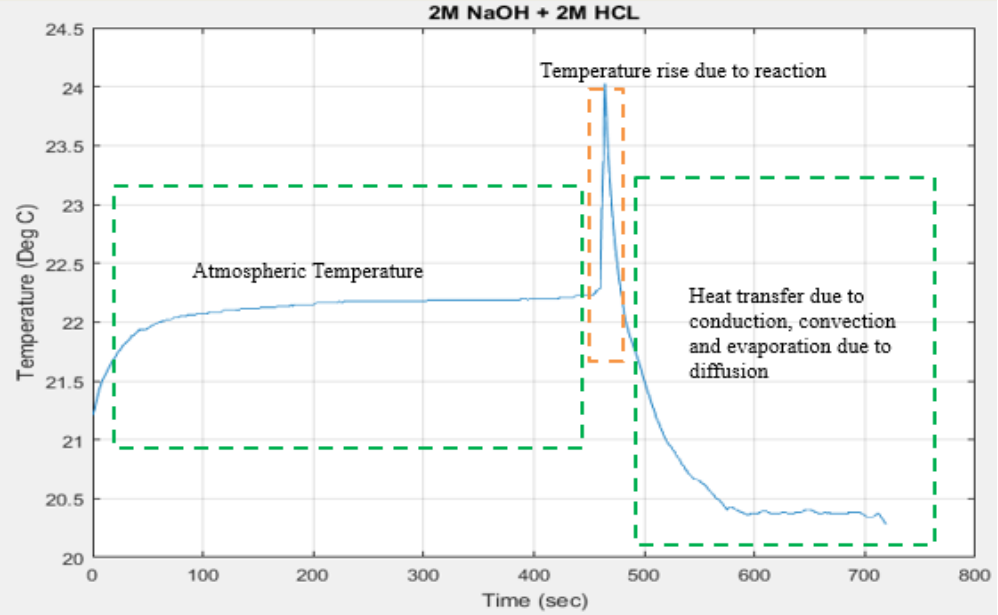

Figure 6-2, Experimental data of 2M HCl + 2M NaOH

Same experiment was carried out with 2M HCL and 2M NaOH as shown in Figure 6-2, that after considerable amount of rise in a temperature due to heat released during reaction, the temperature start dropping gradually with respect to time due to heat conduction from bottom chip and as well as due to heat convection from surface of the droplet. However, it was observed that the temperature of droplet drops below the atmospheric temperature. After proper investigation it was later found that it was due to the evaporation of droplet due to vapor pressure difference, in other words it can be called evaporative cooling. The most probable reason was due to the difference in surface concentration of droplet and water concentration in atmospheric air. Due to the concentration gradient there was a diffusion of water particles into the atmosphere with certain diffusion rate.

To validate the experimental model with numerical model on COMSOL Multiphysics after coupling all three physics the data of temperature versus time were plotted for 100 seconds.

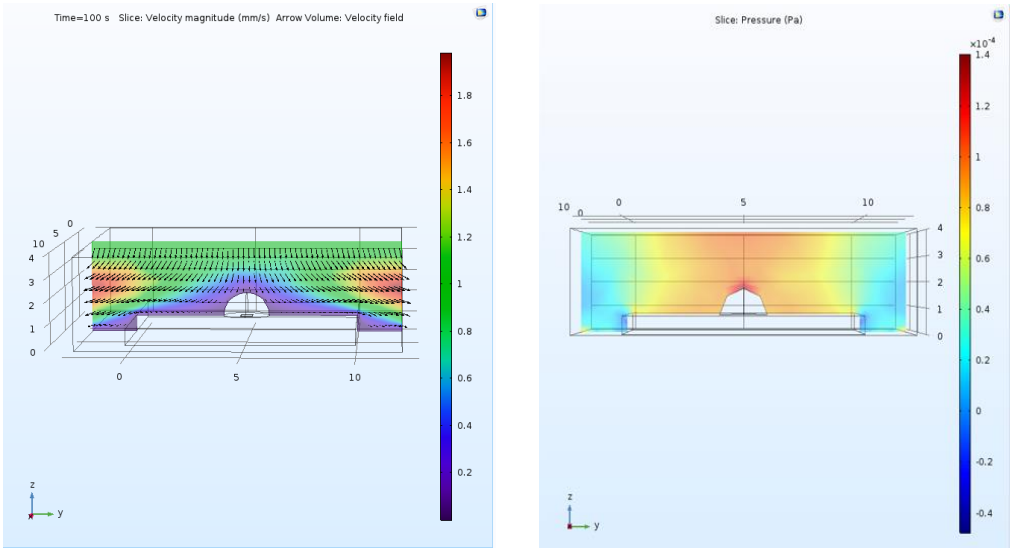

(a) (b)

Figure 6-3 Steady state study 1, (a) Velocity distribution, (b) Pressure distribution

First of all, for study 1 that is steady state simulation was ran for only fluid flow physics and the velocity and pressure values was calculated and it was plotted as shown in Figure 6-3. For next, time dependent study this values of velocity and pressure was used for heat transfer in fluids and transport of diluted species physics.

It can be seen from the Figure 6-3 that the rise in temperature is around 1.6 ^{o}C which is in good accord with the experimental results which shows 1.7 ^{o}C temperature rise of ITO RTD with respect to time.

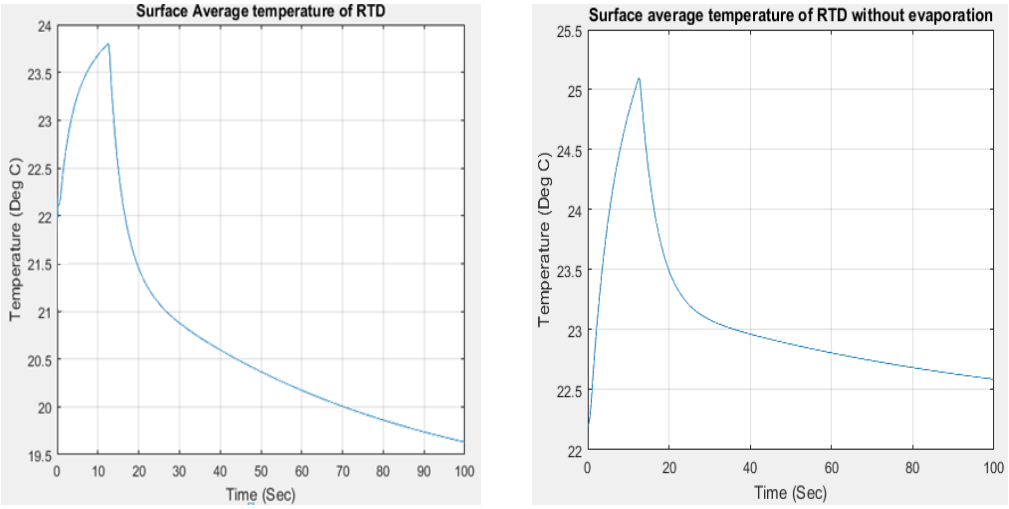

(a) (b)

Figure 6-4 Numerical data of surface temperature of RTD (a) by considering evaporation, (b) without considering evaporation

Again the numerical simulation was also carried out without encountering the evaporation in a given model, which means that diffusion of water particles into the atmosphere was not consider during this part of study. The Figure 6-4 shows the temperature values of RTD with respect to time for 100 sec. It can be understood that without considering evaporation the temperature rises of RTD was 3^{o}C and more importantly temperature doesn't drop below the atmospheric temperature. From this results we can say that the evaporation plays a significant role in heat transfer at micro scale.

As mention earlier in heat transfer in microsystem in chapter 1, due to the low characteristics length the micro droplet was considered as isothermal at any time, but however it was found that due to significant heat loss from the system through conduction, convection and evaporation the droplet will no more remains isothermal. Figure 6-5 shows the slice temperature of droplet at 9 second and 13 second by

considering evaporation in model which relates to actual experimental condition. As mention earlier during 9 second the volumetric heat flux value is on, so at that point of time inside surface of the droplet will be having more temperature compare to outside surface due to evaporation from the very top surface and conduction through the bottom plate. Similarly, at 100 second volumetric heat flux in off and due to evaporation on the surface, temperature of the surface of the droplet drops as shown in Figure 6-5.

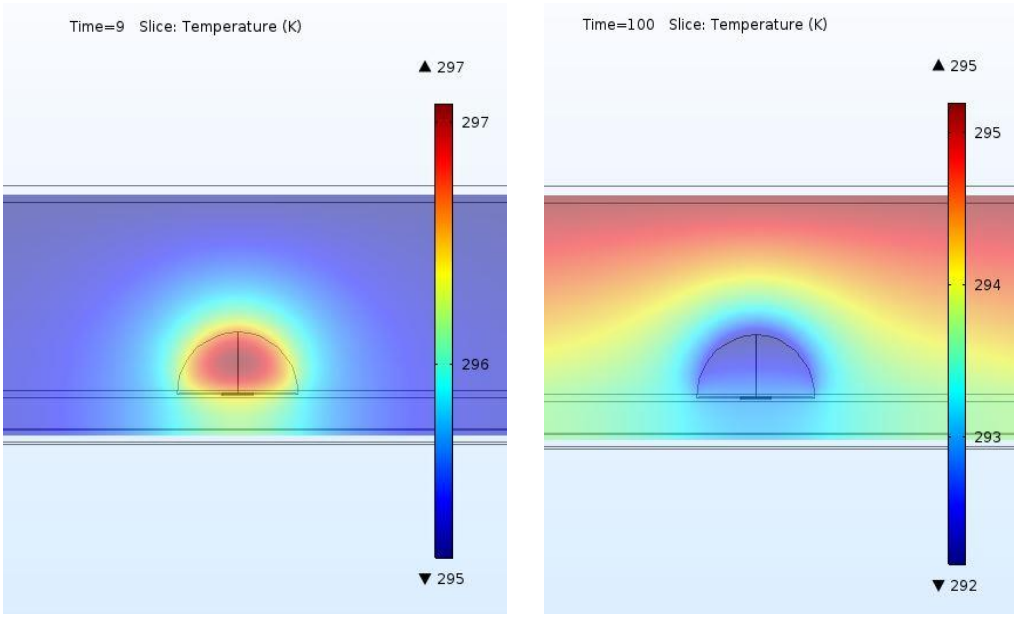

(a) (b)

Figure 6-5 Slice temperature of droplet by considering evaporation at (a) 9 sec, (b) 13 sec

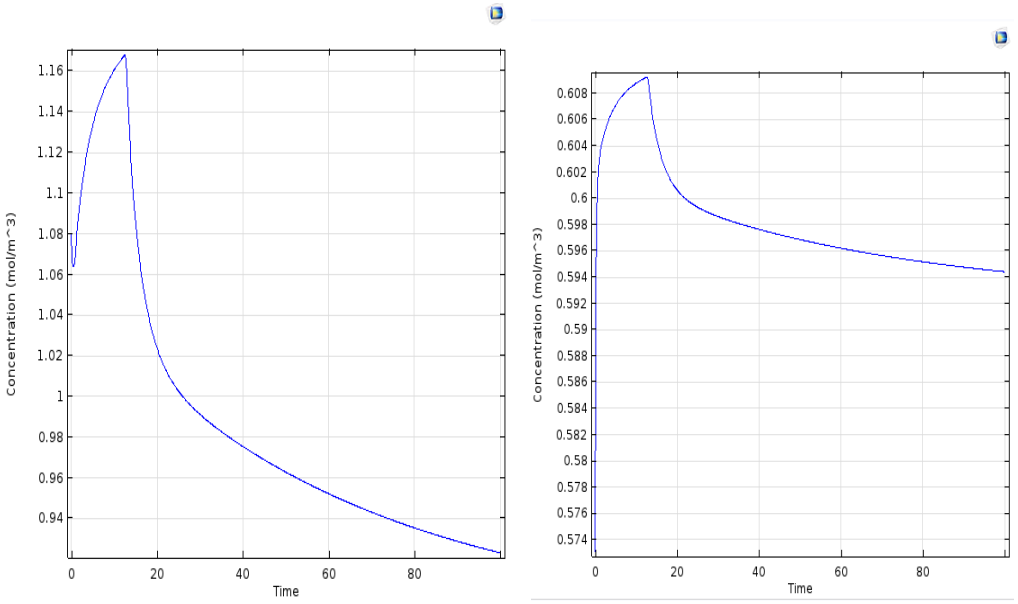

(a) (b)

Figure 6-6, (a) Interfacial Concentration of water in air, (b) volume average concentration of inlet air

Further testament to this fact surface concentration of droplet surface was plotted with respect to temperature as shown in Figure 6-5. From given numerical results it can be interpreted that with increase in temperature the surface concentration increases because saturated boundary condition was applied on the surface of the droplet. So with increase in temperature, saturated pressure also increases which eventually increases interfacial concentration of water in air. Figure 6-5 (b) shows the volume average concentration of air, which shows that average volume concentration of inlet air increases from 0.507 to 0.608 mol/m^3 due to diffusion of water vapor particles in to the air domain due to concentration gradient. After reaching to maximum value 0.609 mol/m^3 theaverage volume concentration again decreases which was due to the continuous flow of air.

Figure 6-6 shows x-z view of droplet relative humidity and concentration contours of air together. It can be seen from this contour that as we move near to droplet, relative humidity as well as concentration increases. The maximum interfacial concentration of water in air at the end of 100 seconds is 0.59 mol/m^3 which is near to the surface of the droplet. The concentration and relative humidity is lower in the region, away from the droplet which is quite reasonable.

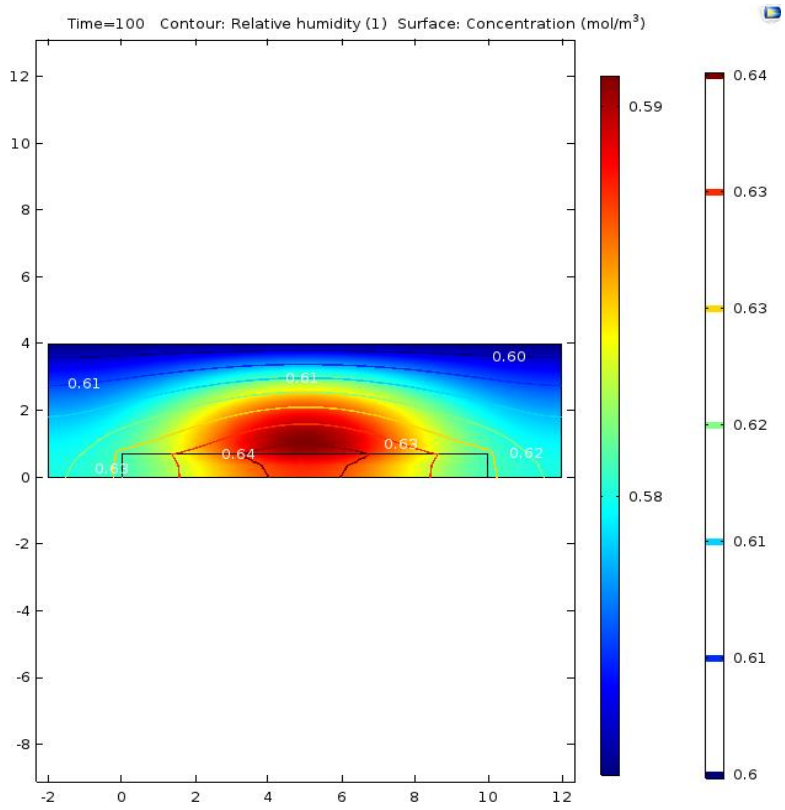

Figure 6-7, Concentration and relative humidity contours of an air domain

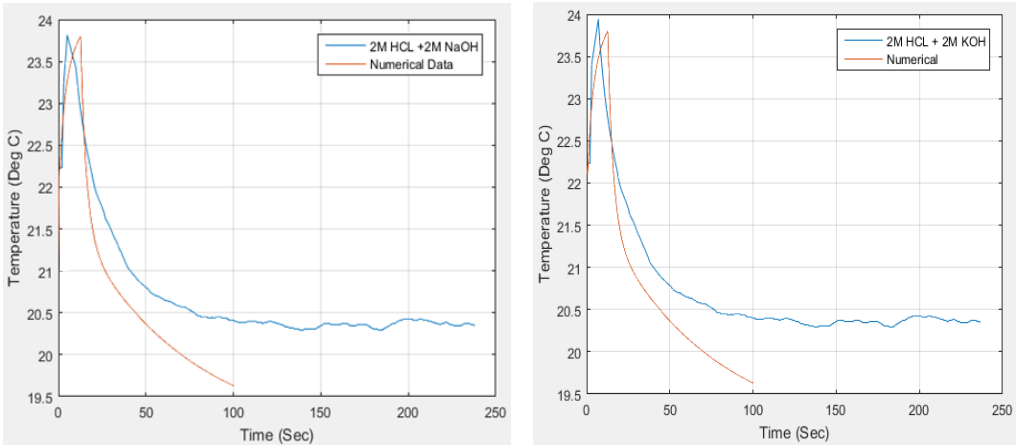

Figure 6-8 Experimental and Numerical results combine

For experimental data validation again experimental and numerical data were plotted together as shown in Figure 6-7. From Figure 6-7 the rise in the temperature in both the case experimental as well as numerical is nearly same but there was a difference in the rate of decrease in the ITO RTD temperature. This was mainly because of the difference in the boundary conditions of the fluid flow, that is difference in velocity as well as direction of inlet air. The another reason could be difference in atmospheric condition like relative humidity and temperature which directly affects the boundary conditions. Again in this numerical model we have assumed droplet as a water, but in an experiment the product will be mixture of salt and water that also affect the rate of decrease in temperature. Also there can be a difference in the diffusion rate of water into the air domain which can also affects the rate of evaporation.

CHAPTER 7 CONCLUSION AND FUTURE WORK

7.1 Conclusion

An experimental and numerical study of heat transfer phenomenon in a micro droplet reactor is carried out. The conclusions drawn from this study is derived:

1) The thin film ITO RTD sensor was able to measure the temperature along the micro droplet reactor of the heat released from the reaction as well as the reaction enthalpy with accuracy of about 5%.
2) Experimental results are in good agreement with the numerical study carried out using COMSOL Multiphysics.
3) At microscale along with conduction and convection evaporation due to vapor pressure gradient plays an important role in heat transfer.

7.2 Future Work

The following work can be done in a future with this study of heat transfer phenomenon in a micro droplet reactor.

1) Temperature monitoring at micro scale can be carried out using embedded ITO RTD in a micro droplet reactor with control environment like a vacuum or low pressure chamber having low velocity of air and high relative humidity.
2) This Numerical model can be useful for the study of hot spot cooling with thin film evaporation.
3) The EWOD device with multiple layers can be used as a micro reactor with temperature sensing as well as heating provision with the help of ITO RTD/heater for endothermic reactions.

REFERENCES

[1] Micro reactor as tools for chemical research by “Xunli Zhang”, “Charlotte wlies”, ”Sarah L Painter”, “Paul Watts”, “Stephen J Haswell”.

[2] Multi- step organic synthesis of four different molecular probes in digital microfluidic devices by “Hee-Kwon Kim, Supin Chen, Muhammad Rashed Javed, Jack Lei, CJ Kim, Pei Yuin Keng, R. Michael van Dam**”** *Dept. of Molecular & Medical Pharmacology; Dept. of Bioengineering; Dept. of Mechanical and Aerospace Engineering University of California, Los Angeles, USA*

[3] G. Bindiganavale, "Study of Hotspot Cooling for Integrated Circuits Using Electrowetting on,” no. May, 2015", Ph.D, The University of Texas at Arlington, 2015.

[4] https://en.wikipedia.org/wiki/Biot_number

[5] R.L. Hartman, K.F. Jensen, Microchemical systems for continuous-flow synthesis, Lab Chip 9 (2009) 2495.

[6] P. Plouffe, A. Macchi, D.M. Roberge, From batch to continuous chemical synthesis—a toolbox approach, Org. Process Res. Dev. 18 (2014) 1286–1294.

[7] W. Navarrini, F. Venturini, V. Tortelli, S. Basak, K.P. Pimparkar, A. Adamo, K.F. Jensen, Direct fluorination of carbon monoxide in microreactors, J. Fluorine Chem. 142 (2012) 19–23.

[8] A.A. Kulkarni, Continuous flow nitration in miniaturized devices, Beilstein J. Org. Chem. 10 (2014) 405–424.

[9] K.T. Zuidhof, M.H.J.M. de Croon, J.C. Schouten, Beckmann rearrangement of cyclohexanone oxime to e-caprolactam in microreactors, AIChE J. 56 (2010) 1297–1304.

[10] J.S. Zhang, K. Wang, Y.C. Lu, G.S. Luo, Beckmann rearrangement in a microstructured chemical system for the preparation of e-caprolactam, AIChE J. 58 (2012) 925–931.

[11] Microfabricated power generation devices, Design and technology by *“Alexander Mitsos, and Paul I Barton”.*

[12] http://www.thermopedia.com/content/585/

[13] Thermal analysis of chemical reactions in microchannels using highly sensitive thin-film heat-flux microsensor by “Houssein Ammara, Bertrand Garnier a, Ahmed Ould el Moctar a, Herve´ Willaime b,Fabrice Monti b, Hassan Peerhossaini “

[14] Realizing Temperature-Controlled Digital Microfluidic Chips with Versatile Microelectrodes by “Jen-Hung Wei, Wen-Syang Hsu and Shih-Kang Fan.” *Department of Mechanical Engineering, National Chiao Tung University, Taiwan Institute of Nanotechnology, National Chiao Tung University, Taiwan*

[15] K. Wang, Y.C. Lu, H.W. Shao, G.S. Luo, Measuring enthalpy of fast exothermal reaction with micro-reactor-based capillary calorimeter, AIChE J. 56 (2009) 1045–1052.

[16] R. Fu, B. Xu, D. Li, Study of the temperature field in microchannels of a PDMS chip with embedded local heater using temperature-dependent fluorescent dye, Int. J. Therm. Sci. 45 (2006) 841–847.

[17] Heat transfer analysis and improved mixing in multifunctional microreactor using sapphire window and infrared thermography by Ammar, Houssein; Garnier, Bertrand; Sediame, Dounia; El Moctar, Ahmed Ould; Peerhossaini, Hassan.

[18] R. Kuriyama, Y. Sato, Non-intrusive measurement of microscale temperature distribution by spontaneous Raman imaging, Microfluid. Nanofluid. 14 (2013) 1031–1037.

[19] A. Ewinger, G. Rinke, A. Urban, S. Kerschbaum, In situ measurement of the temperature of water in microchannels using laser Raman spectroscopy, Chem. Eng. J. 223 (2013) 129–134.

[20] J. Haber, M.N. Kashid, N. Borhani, J. Thome, U. Krtschil, A. Renken, L. Kiwi-Minsker, Infrared imaging of temperature profiles in microreactors for fast and exothermic reactions, Chem. Eng. J. 214 (2013) 97–105.

[21] Measuring enthalpy of fast exothermal reaction with infrared thermography in a microreactor by *“J.S.Zhang”, “C.Y.Zhang”,”G.T.Liu”, “G.S.Luo”. Department of chemical Engineering, Tsinghua university, Beijing china*

[22] P. Yi, A.A. Kayani, A.F. Chrimes, K. Ghorbani, S. Nahavandi, K. Kalantar-zadeh, K. Khoshmanesh, Thermal analysis of nanofluids in microfluidics using an infrared camera, Lab Chip 12 (2012) 2520.

[23] G. Hetsroni, A. Mosyak, E. Pogrebnyak, R. Rozenblit, Infrared temperature measurements in micro-channels and micro-fluid systems, Int. J. Therm. Sci. 50 (2011) 853–868.

[24] An EWOD droplet microfluidic chip with integrated local temperature control for multiplex proteomics by *"Wyatt Nelson", "Ivory Peng", "Joseph A. Loo"," Robin L. Garrell", and "Chang-Jin Kim."*

[25] Experimental and Numerical study of Marangoni convection in a sandwich droplet by "Ajinkya Shetye, University of Texas at Arlington, April 2016".

[26] Casquillas, G.V., Bertholle, F., Le Berre, M., Meance, S., Malaquin, L., Greffet, J.J., Chen, Y., 2008. Thermo-resistance based micro-calorimeter for continuous chemical enthalpy measurements. Microelectron. Eng. 85, 1367–1369.

[27] https://en.wikipedia.org/wiki/Finite_element_method.

[28] Modelling evaporative cooling example available online: https://www.comsol.com/blogs/intro-to-modeling-evaporative-cooling/

.

BIOGRAPHICAL INFORMATION

Chintan Jitendra Gandhi earned his bachelor degree in Mechanical Engineering from Gujarat Technological University, India, in 2013. He joined The University of Texas at Arlington in Spring 2015. He is currently a member of Integrated Micro-Nano fluidic systems laboratory at UTA. His area of research is in digital microfluidics, MEMS fabrication, microscale chemical synthesis and thermal management in electronics.